4504 *J. Phys. Chem. A* **2001,** *105,* 4504−4516

Structures, Intramolecular Rotation Barriers, and Thermochemical Properties of Radicals Derived from H Atom Loss in Mono-, Di-, and Trichloromethanol and Parent Chloromethanols

Hongyan Sun and Joseph W. Bozzelli*

Department of Chemical Engineering, Chemistry and Environmental Science,
New Jersey Institute of Technology, Newark, New Jersey 07102

Received: October 20, 2000; In Final Form: February 28, 2001

Structures and thermochemical properties, ΔH°_{f298}, S°_{298} and $C_p(T)$ of three (mono-, di-, and tri-) chloromethanols; three chloromethoxy and the two hydroxychloromethyl radicals are determined by ab initio and density functional calculations. The molecular structures and vibration frequencies are determined at the B3LYP/6-31G(d,p) density functional level, with single point calculations for the energy at the B3LYP/6-311+G-(3df,2p), QCISD(T)/6-31G(d,p), and CBSQ//B3LYP/6-31G(d,p) levels. The vibration frequencies are scaled for zero-point energies and for thermal corrections. The enthalpies of formation (ΔH°_{f298}) are determined at each calculation level using several isodesmic reactions. Standard entropy (S°_{298}) and heat capacity ($C_p(T)$'s, $300 \leq T/\mathrm{K} \leq 1500$) from vibrational, translational, and external rotational contributions are calculated using the rigid-rotor-harmonic-oscillator approximation based on the vibration frequencies and structures obtained from the density functional study. Potential barriers for internal rotation of the hydroxyl group are calculated at the B3LYP/6-31G(d,p) level, and hindered internal rotational contributions to entropy and heat capacity are calculated by summation over the energy levels obtained by direct diagonalization on the Hamiltonian matrix of hindered internal rotations. An evaluation of data from the isodesmic reactions at each calculation level results in the enthalpy of formation values: -58.07 ± 0.69, -65.88 ± 0.76, and -65.96 ± 0.76 kcal/mol for mono-, di-, and trichloromethanol, respectively. The standard enthalpies for the mono-, di-, and trichloromethoxy radicals are -5.13 ± 2.18, -7.65 ± 2.25, and -9.05 ± 2.24 kcal/mol, respectively. The standard enthalpies for the hydroxymono- and hydroxydichloromethyl radicals are -14.46 ± 1.75 and -22.54 ± 1.83 kcal/mol. Bond energies for the RO−H bond are 105.04, 110.33, and 109.01 kcal/mol, respectively. Bond energies for the R−OH bonds are 95.20, 98.81, and 94.39 kcal/mol, respectively. Groups for use in Benson type additivity estimations are determined for the carbon bonded to oxygen and chlorine(s). The enthalpy values for the C/Cl/H_2/O, C/Cl_2/H/O, and C/Cl_3/O groups are -20.17, -27.98, and -28.06 kcal/mol, respectively. Hydrogen bond increment groups for the chloromethoxy and hydroxychloromethyl radicals are also developed. The bond energies and ΔH°_{f298} values suggest that the electronegative Cl(s) on the methyl serve to increase and RO−H bond energy. ΔH°_{f298} for $C^\bullet H_2OH$, $CH_3C^\bullet HOH$, and $C_2H_5O^\bullet$ are also determined and compared with literature data, and recommended values are -3.97 ± 0.22, -13.34 ± 0.84, and -3.90 ± 1.27 kcal/mol, respectively.

Introduction

Chlorocarbons are widely used chemicals as solvents in synthesis and in cleaning agents, as synthesis starting materials, and in polymer, pesticide, and other product manufacture. Chlorocarbons and other halocarbon compounds are present in the atmosphere from evaporation of these solvents and other anthropogenic activities. They often exhibit relatively long tropospheric lifetimes due to their slow decay or low reaction rates with $OH^\bullet$ radical.[1] If they diffuse into the stratosphere, the chlorine will contribute to the reduction of stratospheric ozone levels. Chlorine substitution on methyl and alkyl radicals results in lower reactivity of the radical with oxygen, and this slower reaction with O_2 permits the chlorinated radicals to build up to higher concentrations in combustion environments. These species are more likely to undergo reactions with the radical pool, of which $HO_2^\bullet$, $OH^\bullet$, and $O^\bullet$ atoms are likely reactants. Association reactions of $CH_2Cl^\bullet$, $CHCl_2^\bullet$, and $CCl_3^\bullet$ with these radicals lead to formation of chloromethanol or chloromethoxy species; the presence of these adducts needs to be considered in modeling the combustion efficiency and pollutant formation.

The thermochemical property data on these oxygenated chlorocarbon species are needed for evaluation of reaction paths and kinetic processes, such as stability of intermediate adducts and prediction of final products. The thermodynamic properties are also needed for use in kinetic modeling and in equilibrium codes. There is limited experimental data on the thermodynamic properties of these oxygenated chlorocarbons in the literature with exception of acid carbonyl (acid chloride) species. This research is an attempt to calculate the fundamental thermodynamic property data on these species using ab initio and density functional calculations with working reactions for cancellation of error.

Several experimental and theoretical studies have been reported on structural and related properties of chloromethanol and chloromethoxy species.[2−7] Kunttu et al.[2] reported vibration frequencies of chloromethanol from infrared spectra; they

---

* Corresponding author. E-mail: Bozzelli@njit.edu.

10.1021/jp003877t CCC: $20.00 © 2001 American Chemical Society

calculated its geometry and vibrational frequencies at the HF/6-31G(d,p) ab initio level. Tyndall et al.[3] reported experimental infrared frequencies, along with calculated frequencies and geometric parameters at the RHF/6-31G(d,p) level for mono- and dichloromethanol. Schneider et al.[4] calculated the structures at the RHF/6-31G(d,p) level and bond energies and heats of formation at MP2/6-31G(d,p) for chlorinated methanols and chloromethoxy radicals. Wallington et al.[5] have recently investigated the stability and infrared spectra of the three chlorinated methanols under atmospheric conditions using smog-chamber experiments. Melius[6] calculated the structures, moments of inertia, and frequencies at the HF/6-31G(d) level of theory, and calculated the enthalpies and the free energies for these species using the BAC-MP4 method. Kinetic studies on thermal decomposition rates under atmospheric conditions, which reflect on species stability, are in disagreement by several orders of magnitude.[7−9] There is also considerable discrepancy in the reported enthalpy data; for example, the respective ΔH°_{f298}'s of mono-, di-, and trichloromethanol are reported to be −58.8, −66.3, and −70.0 kcal/mol by Schneider et al.[4] and they are listed as −55.50, −66.40, and −66.20 kcal/mol by NIST.[6c] There is no published thermochemical property data (S°_{298} and $C_p(T)$) on chloromethoxy or hydroxychloromethyl radicals that we are aware of.

In this work, enthalpy, ΔH°_{f298}, entropy, S°_{298}, and heat capacities, $C_p(T)$, are determined for the three chloromethanols, the corresponding three chloromethoxy radicals, and two hydroxychloromethyl radicals using density functional and ab initio calculation methods. The enthalpies of formation are evaluated at each calculation level, using several isodesmic reactions. Contributions to entropy and heat capacity from internal rotation of the hydroxyl group are estimated using direct integration over energy level of the intramolecular rotation potential energy curve, with the B3LYP/6-31G(d,p) level calculations for rotation barrier estimations. A set of chloro−oxy−hydrocarbon groups and hydrogen bond increment groups are derived from these thermochemical property data.

Calculation Method

All of the density functional and ab initio calculations are performed using the Gaussian94 program suite.[10] The geometry optimization, harmonic vibration frequencies, and zero-point vibrational energies (ZPVE) are computed with the B3LYP/6-31G(d,p) level of theory (opt = verytight are used in calculation for the accurate geometries). The optimized geometry parameters are used to obtain total electronic energies at the B3LYP/6-31G(d,p), B3LYP/6-311+G(3df,2p), QCISD(T)/6-31G(d,p), and CBSQ//B3LYP/6-31G(d,p) (abbreviated as CBSQ//B3**) single point levels of calculation.[11−13] Total energies are corrected by zero-point vibration energies (ZPVE), which are scaled by 0.9806, as recommended by Scott et al.[14] Thermal correction, 0 to 298.15 K, is taken into account using the B3LYP structure and vibration data. The CBSQ calculations include an SCF energy at HF/6-311+G(3d2f,2df,2p), higher order correlation at QCISD(T)/6-31+g(d′), MP4(SDQ)/6-31+G(d(f),d,p), and a further second-order correlation at MP2/6-311+G(3d2f,2df,2p). They are reported to result in an energy value at the QCISD(T)/6-31++G(3df,2p) level of calculation. Restricted and open shell B3LYP/6-31G(d,p) calculations are used for the chloromethanols and radicals, respectively.

Contributions of vibration, translation, and external rotation to entropies and heat capacities are calculated from scaled vibrational frequencies and moments of inertia of the optimized structures. Potential barriers for the internal rotations of hydroxyl group are determined at the B3LYP/6-31G(d,p) calculation level (each conformer and barrier optimized). The geometries and harmonic vibrational frequencies are calculated for all the rotational structures at the B3LYP/6-31G(d,p) level. Contributions from hindered rotor to S°_{298} and $C_p(T)$ are determined using direct integration over energy levels of the intramolecular rotational potential energy curves. The number of optical isomers and the spin degeneracy of unpaired electrons are also incorporated for calculation of S°_{298}.

A truncated Fourier series is used to represent the torsional potential calculated at discrete torsional angles:

$$V(\Phi) = a_0 + \sum a_i \cos(i\Phi) + \sum b_i \sin(i\Phi) \qquad i = 1-5 \tag{F1}$$

where values of the coefficients a_i and b_i are calculated to provide the true minima and maxima of the torsional potentials with allowance of a shift of the theoretical extreme angular positions.[15−17]

Enthalpies of formation (ΔH°_{f298}) for the target species are estimated using total energies and several sets of isodesmic reactions. Reactions in Scheme 1 are used to calculate ΔH°_{f298} of mono-, di-, and trichloromethanol.

SCHEME 1

$$CH_{3-x}Cl_xOH + CH_4 \rightarrow CH_3OH + CH_{4-x}Cl_x \tag{1.1}$$

$$CH_{3-x}Cl_xOH + C_2H_6 \rightarrow C_2H_5OH + CH_{4-x}Cl_x \tag{1.2}$$

$$CH_{3-x}Cl_xOH + C_2H_6 \rightarrow CH_3OH + CH_3CH_{3-x}Cl_x \tag{1.3}$$

$$CH_{3-x}Cl_xOH + C_3H_8 \rightarrow C_2H_5OH + CH_3CH_{3-x}Cl_x \tag{1.4}$$

$$CH_{3-x}Cl_xOH + C_3H_8 \rightarrow n\text{-}C_3H_7OH + CH_{4-x}Cl_x \tag{1.5}$$

Reactions in Scheme 2 are used to calculate ΔH°_{f298} of mono-, di-, and trichloromethoxy radicals.

SCHEME 2

$$CH_{3-x}Cl_xO^\bullet + CH_4 \rightarrow CH_{3-x}Cl_xOH + CH_3^\bullet \tag{2.1}$$

$$CH_{3-x}Cl_xO^\bullet + C_2H_6 \rightarrow CH_{3-x}Cl_xOH + C_2H_5^\bullet \tag{2.2}$$

$$CH_{3-x}Cl_xO^\bullet + CH_4 \rightarrow CH_{4-x}Cl_x + CH_3O^\bullet \tag{2.3}$$

$$CH_{3-x}Cl_xO^\bullet + C_2H_6 \rightarrow CH_{4-x}Cl_x + C_2H_5O^\bullet \tag{2.4}$$

$$CH_{3-x}Cl_xO^\bullet + CH_3OH \rightarrow CH_{3-x}Cl_xOH + CH_3O^\bullet \tag{2.5}$$

$$CH_{3-x}Cl_xO^\bullet + C_2H_5OH \rightarrow CH_{3-x}Cl_xOH + C_2H_5O^\bullet \tag{2.6}$$

Reactions in Scheme 3 are used for ΔH°_{f298} of hydroxy-mono- and hydroxydichloromethyl radicals.

SCHEME 3

$$C^\bullet H_{2-x}Cl_xOH + CH_4 \rightarrow CH_{3-x}Cl_xOH + CH_3^\bullet \tag{3.1}$$

$$C^\bullet H_{2-x}Cl_xOH + C_2H_6 \rightarrow CH_{3-x}Cl_xOH + C_2H_5^\bullet \tag{3.2}$$

$$C^\bullet H_{2-x}Cl_xOH + CH_4 \rightarrow CH_{4-x}Cl_x + C^\bullet H_2OH \tag{3.3}$$

$$C^\bullet H_{2-x}Cl_xOH + C_2H_6 \rightarrow CH_{4-x}Cl_x + CH_3C^\bullet HOH \tag{3.4}$$

$$C^\bullet H_{2-x}Cl_xOH + CH_3OH \rightarrow CH_{3-x}Cl_xOH + C^\bullet H_2OH \tag{3.5}$$

$$C^\bullet H_{2-x}Cl_xOH + C_2H_5OH \rightarrow CH_{3-x}Cl_xOH + CH_3C^\bullet HOH \tag{3.6}$$

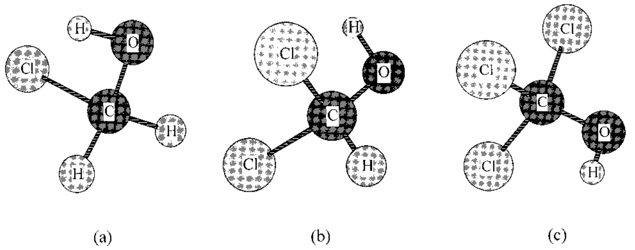

Figure 1. B3LYP/6-31G(d,p) optimized geometries of three chlorinated methanols: (a) chloromethanol; (b) dichloromethanol; (c) trichloromethanol.

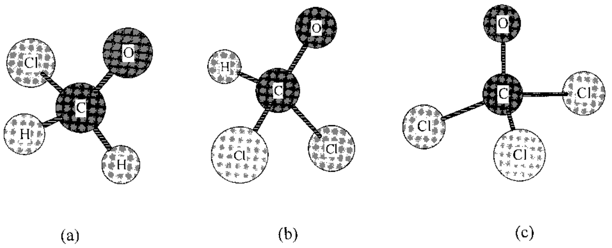

Figure 2. B3LYP/6-31G(d,p) optimized geometries of three chloromethoxy radicals: (a) chloromethoxy radical; (b) dichloromethoxy radical; (c) trichloromethoxy radical.

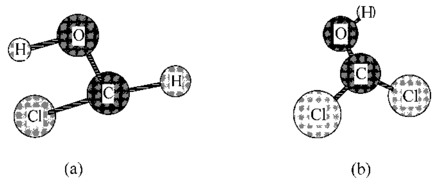

Figure 3. B3LYP/6-31G(d,p) optimized geometries of two hydroxychloromethyl radicals: (a) hydroxychloromethyl radical; (b) hydroxydichloromethyl radical.

The basic requirement of an isodesmic reaction is bond conservation, where the number of each of bond type is conserved in the reaction. An isodesmic reaction will lead to more accurate results if groups are also conserved in the reaction, because the next nearest neighbor interaction is then conserved. Accuracy to near 1 kcal/mol using this method of enthalpy estimation is illustrated in several previous studies.[15,18] Reactions 2.1 and 2.2 are not isodesmic; they are useful for comparison, and for demonstration on the importance of isodesmic reaction. Reactions 2.5 and 2.6 conserve groups in addition to bond types (group isodesmic) and we consider these the best reactions for evaluation of the ΔH°_{f298} as error cancellation should be optimal.

Calculations at each level of theory are performed on the stable conformer(s) of each compound, and the ΔH°_{f298} of each conformer is calculated using isodesmic reactions. Final ΔH°_{f298} values are from a statistical distribution of rotational conformers.

Results and Discussion

Geometry. The fully optimized geometries at the B3LYP/6-31G(d,p) density functional calculation level for mono-, di-, and trichloromethanol are presented in Figure 1, for mono-, di-, and trichloromethoxy radicals in Figure 2, and for hydroxymono- and hydroxydichloromethyl radicals in Figure 3. The numerical values of the structural parameters including carbon−hydrogen, carbon−chlorine, carbon−oxygen, and oxygen−hydrogen bond distances along with applicable bond angles are listed in Tables 1−3, respectively. Comparisons are made to the data computed by Schneider et al.[4] at the RHF/6-31G(d,p) level and to the values computed by Wang et al.[9a] at the UMP2-(full)/6-31G(d) level.

The effects of chlorine α-substitution on molecular geometries can be seen from Scheme 4. The C−O bond length decreases significantly with the first chlorine substitution, moderately with the second Cl, and very little with the third chlorine. The C−O bond decrease in CH_2ClOH and in $CH_2ClO^\bullet$ radical resulting from one Cl addition (ca. 0.04 Å) is similar in magnitude to the decrease, due to resonance, resulting from $C^\bullet H_2OH$ radical formation from methanol.[32]

SCHEME 4

R_{C-O}, Å		R_{C-O}, Å		R_{C-O}, Å	
CH_3OH	1.418	$CH_3O^\bullet$	1.369	$C^\bullet H_2OH$	1.369
CH_2ClOH	1.374	$CH_2ClO^\bullet$	1.315	$C^\bullet HClOH$	1.349
$CHCl_2OH$	1.354	$CHCl_2O^\bullet$	1.302	$C^\bullet Cl_2OH$	1.346
CCl_3OH	1.351	$CCl_3O^\bullet$	1.299		

In contrast, the O−H bond length increases with the increased chlorine substitution (see Scheme 5). The trends in C−O and O−H bond lengths are alsoobserved in the geometries calculated at the RHF/6-31G(d) and UMP2(full)/6-31G(d) levels of theory[4,9] (see Tables 1−3). It is unusual that while the O−H bond length increases, it also gets stronger (see the bond energy discussion below).

SCHEME 5

R_{O-H}, Å		R_{O-H}, Å	
CH_3OH	0.965	$C^\bullet H_2OH$	0.966
CH_2ClOH	0.967	$C^\bullet HClOH$	0.969
$CHCl_2OH$	0.970	$C^\bullet Cl_2OH$	0.970
CCl_3OH	0.971		

The optimized geometries at the B3LYP/6-31G(d,p) level show that CH_3OH, $CHCl_2OH$, and CCl_3OH have C_s symmetry and that CH_2ClOH has C_1 symmetry. Because the internal rotation barrier estimated at the B3LYP/6-31G(d,p) level for CH_3OH and CCl_3OH is low, about 1.4−1.7 kcal/mol, the symmetry for these two species could be considered 1 at low temperature, and 3 at higher temperatures, where internal rotation about the C−OH bond is rapid.

It is interesting to evaluate the density functional structure predictions, planar (sp^2) vs tetrahedral (sp^3), on the hydroxymethyl and hydroxychloromethyl radicals. The H_c−C−O−H_c dihedral angle in $C^\bullet H_2OH$ is 148°, which suggests a structure that is halfway between planar and tetrahedral. The H_c−C−O−Cl dihedral angle in $C^\bullet HClOH$ is 134.9° and the Cl−C−O−Cl dihedral in $C^\bullet Cl_2OH$ is 132.7°, indicating these chlorinated carbon radicals are closer to tetrahedral (see Figure 3 and the data in Table 3). Johnson et al.[32] reported that hydroxymethyl has a nonplanar structure based on the geometry optimized at the MP2/6-311G(2df,2p) level of theory and has unequal C−H bonds within the methylene group. Our density functional calculations show similar trends with the data of Johnson's; but just slightly longer bonds (0.006−0.01 Å); see Table 3. The inversion frequencies for $C^\bullet H_2OH$, $C^\bullet HClOH$, and $C^\bullet Cl_2OH$ are calculated in this work to be 443.4, 364, and 262 cm^{-1}, respectively. The symmetries for $C^\bullet H_2OH$ and $C^\bullet Cl_2OH$ are assigned as 1 on the basis of these data.

The bond angles, where oxygen is the center atom, on the methanol and the hydroxyl methyl radicals are near 109° and suggest a tetrahedral structure for bonds on the O atom. Bair and Goddard[19a] reported a tetrahedral structure for the O in peroxides, with a 140° angle between the oxygen lone pairs on each oxygen atom and a 110° angle between the bond and lone

TABLE 1: Geometric Parameters[a] for CH_3OH, CH_2ClOH, $CHCl_2OH$, and CCl_3OH

	CH_3OH $X_1 = X_2 = H$		CH_2ClOH[b] $X_1 = Cl, X_2 = H$		$CHCl_2OH$ $X_1 = H, X_2 = Cl$		CCl_3OH $X_1 = X_2 = Cl$	
parameter	B3LYP[c]	RHF[d]	B3LYP[c]	RHF[d]	B3LYP[c]	RHF[d]	B3LYP[c]	RHF[d]
$r(C-X_1)$	1.093	1.088	1.088	1.080	1.086	1.073	1.782	1.759
$r(C-X_2)$	1.101	1.082	1.851	1.808	1.824	1.786	1.826	1.784
$r(C-X_2)$	1.101	1.082	1.093	1.076	1.824	1.786	1.826	1.784
$r(C-O)$	1.418	1.398	1.374	1.363	1.354	1.346	1.351	1.344
$r(O-H)$	0.965	0.942	0.967	0.944	0.970	0.947	0.971	0.948
$\angle(O-C-X_1)$	106.9	107.3	108.2	112.3	109.0	108.7	107.2	107.2
$\angle(O-C-X_2)$	112.8	112.1	112.9	108.3	112.4	111.9	111.3	110.8
$\angle(O-C-X_2)$	112.8	112.1	114.4	113.5	112.4	111.9	111.3	110.8
$\angle(H-O-C)$	107.9	109.6	108.9	110.6	109.5	111.1	108.9	110.4
$\angle(X_1-C-O-H)$	180.0	180.0	67.8	65.2	180.0	180.0	180.0	180.0
$\angle(X_2-C-O-H)$	61.5		−175.6		61.6		59.9	
$\angle(X_2-C-O-H)$	−61.5		−51.0		−61.6		−59.9	

[a] Distances in angstroms and angles in degrees. X_1 is the symmetry-unique substituent (H, or Cl) under C_s symmetry; X_2 are the two symmetry equivalent substituents. [b] C_1 symmetry. [c] Geometrical parameters optimized at the B3LYP/6-31G(d,p) level of theory. [d] Geometrical parameters optimized at the RHF/6-31G(d,p) level of theory by Schneider et al.

TABLE 2: Geometric Parameters[a] for $CH_3O^\bullet$, $CH_2ClO^\bullet$, $CHCl_2O^\bullet$, and $CCl_3O^\bullet$

	$CH_3O^\bullet$ $X_1 = X_2 = H$		$CH_2ClO^\bullet$ $X_1 = Cl, X_2 = H$		$CHCl_2O^\bullet$ $X_1 = H, X_2 = Cl$		$CCl_3O^\bullet$ $X_1 = X_2 = Cl$	
parameter	B3LYP[b]	UHF[c]	B3LYP[b]	UHF[c]	B3LYP[b]	UHF[c]	B3LYP[b]	UHF[c]
$r(C-O)$	1.368	1.382	1.315	1.349	1.302	1.346	1.299	1.351
$r(C-X_1)$	1.103	1.088	1.852	1.796	1.109	1.081	1.858	1.771
$r(C-X_2)$	1.110	1.086	1.105	1.082	1.828	1.774	1.805	1.766
$\angle(O-C-X_1)$	113.7	111.7	116.9	113.8	105.6	106.1	97.6	111.8
$\angle(O-C-X_2)$	105.4	106.2	110.6	109.1	114.8	111.8	114.5	106.6
$\angle(X_1-C-X_2)$	110.9		105.4		105.4		109.1	
$\angle(X_2-C-X_2)$	106.2		107.5		109.7		110.1	

[a] Distances in angstroms and angles in degrees. X_1 is the symmetry-unique substituent (H, or Cl) under C_s symmetry; X_2 are the two symmetry equivalent substituents. [b] Geometrical parameters optimized at the B3LYP/6-31G(d,p) level of theory. [c] Geometrical parameters optimized at the UHF/6-31G(d,p) level of theory by Schneider et al.

TABLE 3: Geometric Parameters[a] for $C^\bullet H_2OH$, $C^\bullet HClOH$, and $C^\bullet Cl_2OH$

	$C^\bullet H_2OH$ $X_1 = X_2 = H$		$C^\bullet HClOH$ $X_1 = Cl, X_2 = H$		$C^\bullet Cl_2OH$ $X_1 = X_2 = Cl$	
parameter	B3LYP[b]	MP2[c]	B3LYP[b]	UMP2[d]	B3LYP[b]	UMP2[e]
$r(C-O)$	1.369	1.363	1.349	1.356	1.346	1.354
$r(C-X_1)$	1.083	1.075	1.775	1.744	1.788	1.751
$r(C-X_2)$	1.088	1.078	1.086	1.083	1.743	1.718
$r(O-H)$	0.966	0.958	0.969	0.975	0.970	0.968
$\angle(O-C-X_1)$	112.9	113.4	117.0	117.2	115.4	115.7
$\angle(O-C-X_2)$	118.7	118.8	113.0	112.1	111.6	111.4
$\angle(X_1-C-X_2)$	119.9	120.5	113.2		115.5	
$\angle(H-O-C)$	108.9	108.4	109.5	108.9	108.6	107.9
$\angle(X_1-C-O-H)$	176.0		46.0		−45.8	
$\angle(X_2-C-O-H)$	27.8		−179.8		179.7	
$\angle(X_1-C-O-X_2)$	−147.7		134.9		−132.7	

[a] Distances in angstroms and angles in degrees. [b] Geometrical parameters optimized at the B3LYP/6-31G(d,p) level of theory. [c] Geometrical parameters optimized at the MP2/6-311G(2df,2p) level of theory by Johnson et al.[32] [d] Geometrical parameters optimized at the UMP2(full)/6-31G(d) level of theory by Wang et al.[9a] [e] Geometrical parameters optimized at the UMP2=FU/6-31G(d,p) level of theory by Hou et al.[9b]

pair. This phenomenon is also observed in the structures of chlorinated methyl hydroperoxides by Sun et al.[18]

The lowest energy conformation for the three chlorinated methanols consistently has the hydroxyl hydrogen gauche to the maximum number of chlorine atoms as illustrated in Figure 1 and Table 1, despite an apparent steric penalty. Schneider et al.[4] report that this results from a maximizing of the interaction between the unhybridized oxygen π orbital and chlorine(s). Omoto et al.[19b] ascribe this preference (anomeric effect) in CH_2ClOH, to the delocalization of the lone pair electron on the oxygen with the antibonding σ^* orbital of the C−Cl bond. They report the orbital of oxygen with pure p-character interacts with the C−Cl σ^* orbital over a relatively wide range of Cl−C−O−H dihedral angle ($\varphi = 30-150°$) (rotate Cl into H about the C−O bond). The p-character of the oxygen atom lone-pair orbital is close to 100% over this range of dihedral angle.[19b] Whereas a hybrid of the s and p atomic orbitals interacts with the C−Cl orbital in the conformation with ($\varphi = 180°$), here the electron delocalization is suppressed. Consideration of the electrostatic repulsion between the nonbonding electron pair of oxygen and electronegative Cl atom(s) also seems to support this gauche structure. The distances between a hydroxyl hydrogen atom and a chlorine atom on the methyl group are close enough for some electrostatic interaction (2.8 Å)[20] and are less than the sum of the van der Waals radii of H and Cl (3.0 Å).[21] The interatomic distances between the hydroxyl

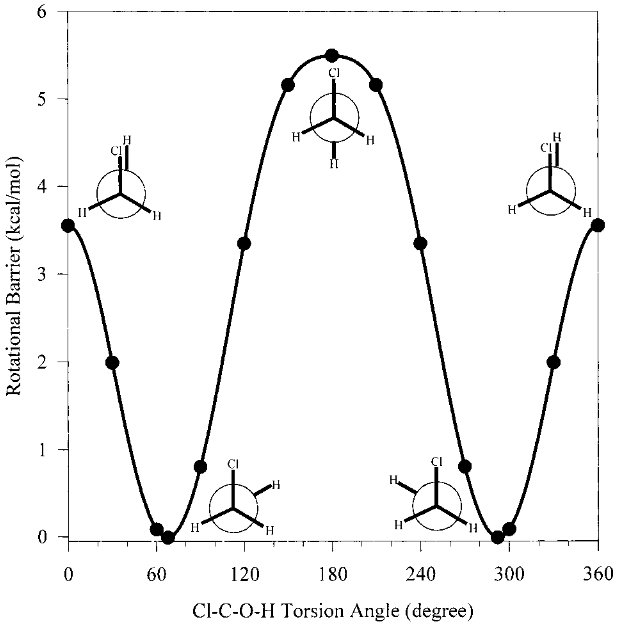

Figure 4. Potential barriers for internal rotation about the C−O bond of CH_2ClOH. Points are calculated values at the B3LYP/6-31G(d,p) level of theory. The line is the Fourier expansion, F1, with the coefficients listed in the Supporting Information (Table S2). The geometries at the points of the minima and maxima are fully optimized.

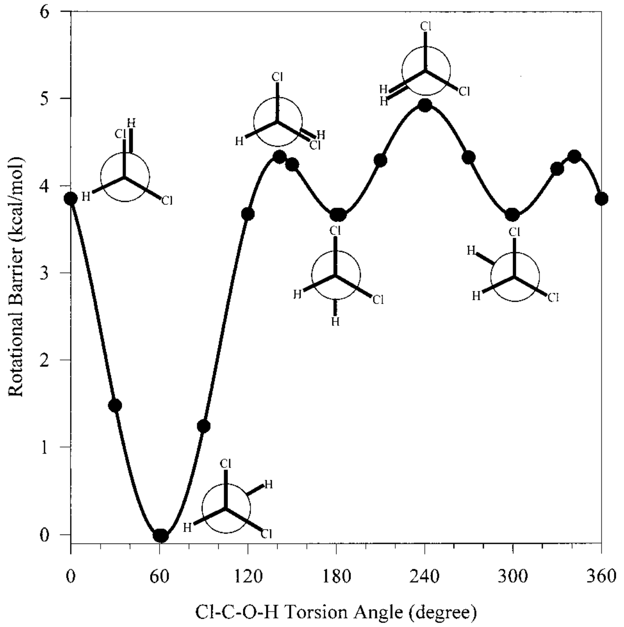

Figure 5. Potential barriers for internal rotation about the C−O bond of $CHCl_2OH$. Points are calculated values at the B3LYP/6-31G(d,p) level of theory. The line is the Fourier expansion, F1, with the coefficients listed in the Supporting Information (Table S2). The geometries at the points of the minima and maxima are fully optimized.

hydrogen and chlorine(s) are 2.893 Å in CH_2ClOH, 2.799 and 2.803 Å in $CHCl_2OH$, and 2.756 and 2.757 Å in CCl_3OH, respectively.

Rotational Barrier. *Chloromethanols.* Potential barriers for internal rotations of CH_2ClOH, $CHCl_2OH$, CCl_3OH, $C^{\bullet}HClOH$, and $C^{\bullet}Cl_2OH$ are calculated at the B3LYP/6-31G(d,p) level. Calculation of potential energy as function of dihedral angle is performed by varying the torsion angle in 30° intervals and allowing the remaining molecular structure parameters to be optimized (except the 0° point in $C^{\bullet}HClOH$ radical, where the dihedral Cl−C−O−H is frozen). Each minimum and maximum on the torsional potential is fully optimized. The geometries and harmonic vibrational frequencies are calculated for all of the rotational structures at the B3LYP/6-31G(d,p) level. The barriers for internal rotations are calculated from the differences between the total energy of each conformation and that of the most stable conformer, where the zero-point vibrational energy (ZPVE) and thermal correction to 298 K are also included. Data on total energies, ZPVE, and thermal correction to 298 K, and calculated rotation barriers for each rotational conformer of the three chlorinated methanols and two hydroxychloromethyl radicals are presented in the Supporting Information (Table S1). Potential barrier diagrams for internal rotations about the C−O bond of above species are shown in Figures 4−8. Points are calculated values at the B3LYP/6-31G(d,p) level. Lines are results of the Fourier expansion F1. The coefficients of the Fourier expansion components, a_i and b_i, in eq F1 are listed in the Supporting Information (Table S2). The stable conformers, as noted below, are calculated at all theory levels.

The calculated rotational barrier for chloromethanol is shown in Figure 4. The H−Cl gauche conformer is the most stable. The H−Cl eclipsed structure with an energy of 3.56 kcal/mol is more stable than the H−Cl anti structure, which has the highest energy, 5.50 kcal/mol. The H−Cl anti structure has a nonbonding e^- pair (from oxygen) gauche to the Cl atom. The H−Cl eclipsed structure has the nonbonding oxygen e^- pair eclipsed with H atoms, and the H−Cl gauche conformer has only an oxygen nonbonding e^- pair−Cl gauche interaction.

Figure 5 shows the calculated rotational barriers in dichloromethanol. The H−H eclipsed structure has a slightly higher energy, 4.94 kcal/mol, than the H−Cl eclipsed structure, 4.32 kcal/mol. The H−H eclipsed structure has the oxygen's nonbonding e^- pair eclipsed with the two Cl atoms, while the H−Cl eclipsed structure allows for possible H bonding (interatomic distance between the Cl atom and the hydroxyl H is 2.520 Å) and has only one e^- pair eclipsed with Cl. The H−H anti conformer has two gauche interactions of oxygen e^- pairs with Cl and is 3.68 kcal/mol lower than the H−Cl anti conformer, which has three e^- pair−gauche interactions with Cl. The energy difference calculated at the B3LYP/6-311+G(3df,2p), QCISD(T)/6-31G(d,p), and CBSQ//B3LYP/6-31G(d,p) levels is in good agreement: 2.98, 3.11, and 2.94 kcal/mol, respectively. CBSQ values are used in the calculation of conformer distributions. These results indicate a gauche interaction between a Cl atom and an O atom nonbonding e^- pair increases energy in the molecule by about 3 kcal/mol.

The calculated rotational barrier for trichloromethanol is shown in Figure 6. The H−Cl eclipsed structure has the energy of 1.82 kcal/mol above the H−Cl gauche conformer, which is the most stable conformer. Three chlorine atoms on the methyl result in a symmetric, 3-fold, rotation barrier about the C−O bond, and all stable conformers have four chlorine gauche interactions with oxygen nonbonding e^- pairs. This increases the H−Cl gauche conformer energy and results in a relatively low internal rotation barrier for trichloromethanol compared to the mono- and dichloromethanol.

Hydroxymethyl Radicals. Figure 7 shows the calculated rotational barriers for the hydroxychloromethyl radical. The H−H anti structure is the most stable conformer; it is 3.25 kcal/mol lower than the H−Cl anti conformer. The energy differences calculated at the B3LYP/6-311+G(3df,2p), QCISD(T)/6-31G(d,p), and CBSQ//B3LYP/6-31G(d,p) levels are 2.37, 2.65, and 2.08 kcal/mol, respectively. The H−Cl anti conformer of $C^{\bullet}$-

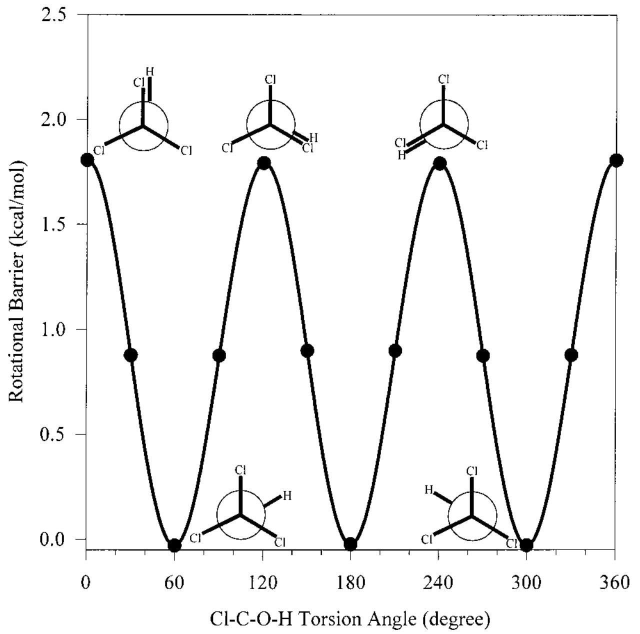

Figure 6. Potential barriers for internal rotation about the C−O bond of CCl_3OH. Points are calculated values at the B3LYP/6-31G(d,p) level of theory. The line is the Fourier expansion, F1, with the coefficients listed in the Supporting Information (Table S2). The geometries at the points of the minima and maxima are fully optimized.

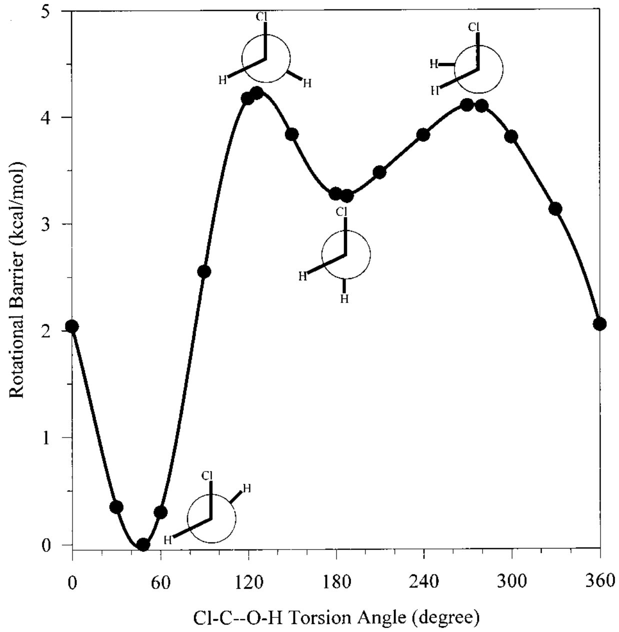

Figure 7. Potential barriers for internal rotation about the C−O bond of $C^{\bullet}HClOH$. Points are calculated values at the B3LYP/6-31G(d,p) level of theory. The line is the Fourier expansion, F1, with the coefficients listed in the Supporting Information (Table S2). The geometries at the points of the minima and maxima are fully optimized except the point of the Cl−C−O−H dihedral at 0°, at which the Cl−C−O−H dihedral is frozen.

HClOH has two nonbonding e^- pairs from the oxygen atom gauche to the Cl atom, while the H−H anti conformer has only one oxygen e^- pair gauche to the Cl atom. The structure with the oxygen atom nonbonding e^- pair eclipsed with the Cl shows the maximum for rotational barrier at 4.22 kcal/mol above the H−H anti minimum. The geometry with the Cl−C−O−H torsion angle 126.1° (see Figure 7) has an energy 0.12 kcal/mol higher than that of the structure with Cl−C−O−H torsion angle 270.0°.

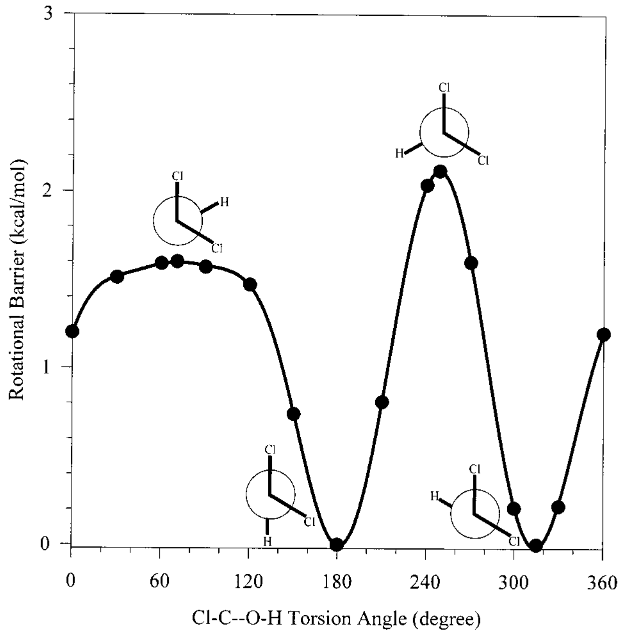

Figure 8. Potential barriers for internal rotation about the C−O bond of $C^{\bullet}Cl_2OH$. Points are calculated values at the B3LYP/6-31G(d,p) level of theory. The line is the Fourier expansion, F1, with the coefficients listed in the Supporting Information (Table S2). The geometries at the points of the minima and maxima are fully optimized.

The calculated rotational potential curve for hydroxydichloromethyl radical is shown in Figure 8. The two low-energy structures have the hydroxyl H anti to one Cl and gauche to one Cl. The structure with a Cl−C−O−H torsion angle of 70.6° is calculated to have an energy 0.52 kcal/mol lower than the structure with a Cl−C−O−H torsion angle of 248.5°. The two H−Cl anti conformers both have three chlorine gauche interactions with oxygen nonbonded electron pairs. This increases the H−Cl anti conformer's energy and provides some explanation why the barrier for C−O internal rotation decreases from 4.22 kcal/mol in $C^{\bullet}HClOH$ to 2.12 kcal/mol in $C^{\bullet}Cl_2OH$.

Enthalpy of Formation (ΔH°_{f298}). The total energies determined at the B3LYP/6-31G(d,p), B3LYP/6-311+G(3df,2p), QCISD(T)/6-31G(d,p), and CBSQ//B3LYP/6-31G(d,p) levels, scaled ZPVE's, and thermal corrections to 298.15 K are listed in Table 4. The spin expectation values, $\langle S^2\rangle$, for $CH_3O^{\bullet}$, $CH_2ClO^{\bullet}$, $CHCl_2O^{\bullet}$, and $CCl_3O^{\bullet}$ are 0.760, 0.761, 0.763, and 0.777, respectively. The values of $\langle S^2\rangle$ for $C^{\bullet}H_2OH$, $C^{\bullet}HClOH$, and $C^{\bullet}Cl_2OH$ are 0.7615, 0.7617, and 0.7630, respectively. Spin contamination is low, and values increase slightly with increased chlorine substitution.

Enthalpies of formation (ΔH°_{f298}) and their respective uncertainties, for standard species used in the working reactions, are adopted from evaluation of literature data or from this work; values are listed in Table 5. The reaction enthalpies and ΔH°_{f298}'s for mono-, di-, and trichloromethanol; mono-, di-, and trichloromethoxy radicals; and hydroxychloromethyl and hydroxydichloromethyl radicals obtained from use of the reaction schemes are tabulated in Tables 7 and 9, respectively.

Reference Data of Radicals in Working Reactions. The selection of the ΔH°_{f298} values for several reference species in the above reaction schemes is important to our determined values. An experimental ΔH°_{f298} of $C^{\bullet}H_2OH$, −2.9 ± 1.0 kcal/mol, has been reported by Berkowitz et al.,[31] and more recently from the same laboratory, −3.97 ± 0.22 kcal/mol by Ruscic et al.[34a] Calculated data are −4.25 ± 0.31 kcal/mol from Johnson et al.,[32] −3.82 kcal/mol from Mayer et al.,[33] and −3.97 ± 0.31

TABLE 4: Total Energies[a] at 0 K

	B3LYP/6-31G(d,p)	/B3LYP6-311+G(3df,2p)	QCISD(T)/6-31G(d,p)	CBSQ//B3LYP/6-31G(d,p)	ZPVE[b]	therm corr[c]
CH_2ClOH	−575.3265536	−575.4076554	−574.4501957	−574.7034556	26.74	2.91
$CHCl_2OH$	−1034.9193506	−1035.0341002	−1033.4813828	−1033.8652102	20.96	3.40
CCl_3OH	−1494.4974476	−1494.6473552	−1492.5005970	−1493.0177223	14.34	4.12
$CH_2ClO^{\bullet}$	−574.6564977	−574.7343632	−573.7816066	−574.0369982	17.40	2.78
$CHCl_2O^{\bullet}$	−1034.2413374	−1034.3533414	−1032.8052066	−1033.1903499	11.89	3.33
$CCl_3O^{\bullet}$	−1493.8235872	−1493.9707796	−1491.8271236	−1492.3450579	6.20	4.08
$C^{\bullet}HClOH$	−574.6650211	−574.7464656	−573.7932899	−574.0528442	18.45	2.88
$C^{\bullet}Cl_2OH$	−1034.2567989	−1034.3727315	−1032.8233922	−1033.2146169	12.78	3.44

[a] Total energy calculation is based on the geometries optimized at the B3LYP/6-31G(d,p) level of theory. Units in Hartree. [b] ZPVE: scaled zero-point energies in kcal/mol. ZPVE is scaled by 0.9806 (Scott and Radom). [c] therm corr: Thermal corrections in kcal/mol.

TABLE 5: ΔH°_{f298} for Species in Reaction Schemes and Bond Energy Calculation[a]

species	ΔH°_{f298}(kcal/mol)	species	ΔH°_{f298} (kcal/mol)
CH_4	$-17.89^{b} \pm 0.07$	$CH_3^{\bullet}$	34.82 ± 0.2^{g}
CH_3Cl	$-19.60^{c} \pm 0.12$	$C_2H_5^{\bullet}$	28.80 ± 0.50^{g}
CH_2Cl_2	$-22.83^{b} \pm 0.29$	$C^{\bullet}H_2OH$	-3.97 ± 0.22^{h}
$CHCl_3$	$-24.20^{d} \pm 0.31$	$CH_3C^{\bullet}HOH$	-13.34 ± 0.84^{i}
CH_3OH	$-48.08^{d} \pm 0.05$	$CH_3O^{\bullet}$	4.10 ± 1.0^{j}
C_2H_6	$-20.24^{d} \pm 0.12$	$C_2H_5O^{\bullet}$	-3.90 ± 1.27^{i}
CH_3CH_2Cl	$-26.84^{c} \pm 0.26$	$CH_2Cl^{\bullet}$	27.70 ± 2.0^{k}
CH_3CHCl_2	$-31.09^{c} \pm 0.29$	$CHCl_2^{\bullet}$	23.50^{l}
CH_3CCl_3	$-34.01^{c} \pm 0.41$	$CCl_3^{\bullet}$	19.00 ± 2^{g}
C_2H_5OH	$-56.12^{d} \pm 0.2$	$Cl^{\bullet}$	28.92 ± 0.3^{g}
C_3H_8	-25.02 ± 0.12^{e}	$H^{\bullet}$	52.10 ± 0.001^{g}
n-C_3H_7OH	-60.97 ± 0.12^{f}	$OH^{\bullet}$	9.43 ± 0.3^{g}

[a] The uncertainties without superscript are evaluated from refs 22 and 23. [b] Reference 24. [c] Reference 25. [d] Reference 28. [e] Reference 22. [f] Reference 26. [g] Reference 27. [h] Reference 33. [i] Estimated in this work. [j] Reference 30. [k] Reference 34b. [l] Reference 34c.

TABLE 6: Reaction Enthalpies and Enthalpies of Formation of $C^{\bullet}H_2OH$, $CH_3C^{\bullet}HOH$, and $C_2H_5O^{\bullet}$ Radicals[a]

reaction series	ΔH°_{rxn} (kcal/mol)	ΔH°_{f298} (kcal/mol)
$C^{\bullet}H_2OH+C_2H_6 \rightarrow C_2H_5^{\bullet}+CH_3OH$	4.91	−3.95
$C^{\bullet}H_2OH+C_2H_5OH \rightarrow CH_3C^{\bullet}HOH+CH_3OH$	−1.31	−3.99
average value and deviation		−3.97 ± 1.11
$CH_3C^{\bullet}HOH+CH_3OH \rightarrow C^{\bullet}H_2OH + C_2H_5OH$	1.31	−13.32
$CH_3C^{\bullet}HOH + CH_4 \rightarrow C^{\bullet}H_2OH + C_2H_6$	7.04	−13.36
av value and deviation		−13.34 ± 0.84
$C_2H_5O^{\bullet}+ CH_3OH \rightarrow CH_3O^{\bullet}+ C_2H_5OH$	−0.06	−3.88
$C_2H_5O^{\bullet}+ CH_4 \rightarrow CH_3O^{\bullet}+C_2H_6$	5.67	−3.92
average value and deviation		−3.90 ± 1.27

[a] The reaction enthalpies and ΔH°_{f298} are calculated at the CBSQ//B3** level.

kcal/mol from Dóbé et al.[35]. In this work, the ΔH°_{f298} for $C^{\bullet}H_2OH$ is calculated to be −3.97 ± 1.11 kcal/mol through analysis of two working isodesmic reactions at the CBSQ//B3** level; this is identical with Ruscic and with Dóbé et al.'s value, and we select −3.97 ± 0.22 kcal/mol as the ΔH°_{f298} of $C^{\bullet}H_2OH$. This corresponds to H−CH_2OH bond energy of 96.2 kcal/mol.

Experimental values of $CH_3C^{\bullet}HOH$ enthalpy are reported as −15.2 ± 1.0 kcal/mol by Alfassi et al.[36] and −14.5 ± 3 kcal/mol by Holmes et al.[37] A calculated value estimated at the G2 level by Dyke et al.[38a] is −13.6 ± 0.9 kcal/mol, and another is −13.58 kcal/mol by Armstrong and Rauk.[38b] In this work, the ΔH°_{f298} of $CH_3C^{\bullet}HOH$ is calculated to be −13.34 ± 0.84 kcal/mol at the CBSQ//B3** level. This is in good agreement with Dyke et al.'s and Armstrong and Rauk's values. We use our value, −13.34 kcal/mol, as the ΔH°_{f298} of $CH_3C^{\bullet}HOH$, which corresponds to a $CH_3CH(OH)$−H bond energy of 94.9 kcal/mol.

An experimental value of ΔH°_{f298} of $C_2H_5O^{\bullet}$, −3.7 ± 0.8 kcal/mol, is reported by Ervin et al.;[39] while calculated values are reported as −3.1 kcal/mol by Curtiss et al.,[40] −3.34 kcal/mol by Yamada et al.,[41] −4 kcal/mol from Benson,[42] and −4.1 kcal/mol by Jungkamp et al.[43] In this work, the ΔH°_{f298} of $C_2H_5O^{\bullet}$ is calculated as −3.90 ± 1.27 kcal/mol at the CBSQ//B3** level, and we use this as the ΔH°_{f298} of $C_2H_5O^{\bullet}$. The resulting CH_3CH_2O−H bond enthalpy is 104.3 kcal/mol, in good agreement with accepted values of 104 kcal/mol.

The ΔH°_{f298} values for the above three species, the working isodesmic reactions and data for calculated values of ΔH°_{rxn} are given in Table 6. The error limits for these three species are calculated by adding the deviations between the isodesmic reactions and the maximum uncertainties in the ΔH°_{f298} of reference species.

Chloromethanol. The results in Table 7 on standard enthalpies show very good consistency for monochloromethanol over the five reactions and the four calculation methods, where the overall average (all reactions and all calculation levels) is −58.54 kcal/mol with a standard deviation of 0.74 kcal/mol. This value is that of the lowest energy, pure enantiomer. The average over the five reaction sets at the CBSQ level is −58.07 ± 0.69 kcal/mol. The 6-311+G(3df,2p) density functional calculation consistently shows slightly higher enthalpy values than the 6-31G(d,p). CBSQ//B3LYP/6-31G(d,p) is the highest level and appears to be the best calculation method for the three chlorinated methanols based on the results for the five reaction series.

Di- and Trichloromethanols. The results for the density functional and QCISD(T) calculations show higher overall deviations than for the monochloromethanol, but still reasonable agreement. The CBSQ//B3** enthalpy values derived by reaction series 1, 2, and 5 show deviation within 0.07 kcal/mol for all three chloromethanols. In contrast, the CBSQ enthalpy values derived in reaction series 3 and 4 differ by up to 2.6 and 2.8 kcal/mol for di- and trichloromethanol relative to values from reaction series 1, 2, and 5. The chemical environment on the carbon with the chlorines changes from an OH to a methyl group in reactions 3 and 4 and changes from an OH to an H atom in 1, 2, and 5. The results from the density functional and QCISD(T) calculations are more consistent with the CBSQ values for reactions 1, 2, and 5.

The choice of CBSQ results from reactions 1, 2, and 5 is further validated by several additional reaction analyses, but now using the enthalpy of chloromethanol, a species determined in this work; see Table 8. The four reaction sets in Table 8 and all calculation levels show reasonable agreement. The enthalpy of dichloromethanol from these additional analysis are −65.79 ± 0.12 kcal/mol, only 0.13 kcal/mol lower than the selected values in Table 7. The average values for trichloromethanol show a slightly higher variation with an average ΔH°_{f298} of

TABLE 7: Reaction Enthalpies at 298 K and Calculated Enthalpies of Formation[a]

	B3LYP/6-31G(d,p)		B3LYP/6-311+G(3df,2p)		QCISD(T)/6-31G(d,p)		CBSQ//B3LYP/6-31G(d,p)	
reaction series	ΔH°_{rxn}	ΔH°_{f298}	ΔH°_{rxn}	ΔH°_{f298}	ΔH°_{rxn}	ΔH°_{f298}	ΔH°_{rxn}	ΔH°_{f298}
1. $CH_2ClOH + CH_4 \rightarrow CH_3OH + CH_3Cl$	9.20	−58.99	8.29	−56.37	8.33	−58.12	8.26	−58.05
2. $CH_2ClOH + C_2H_6 \rightarrow C_2H_5OH + CH_3Cl$	3.73	−59.21	3.31	−58.79	2.77	−58.25	2.54	−58.02
3. $CH_2ClOH + C_2H_6 \rightarrow CH_3OH + CH_3CH_2Cl$	5.21	−59.89	4.17	−58.85	3.91	−58.59	3.26	−57.94
4. $CH_2ClOH + C_3H_8 \rightarrow C_2H_5OH + CH_3CH_2Cl$	1.35	−59.29	0.91	−58.85	0.56	−58.50	0.30	−58.24
5. $CH_2ClOH + C_3H_8 \rightarrow n\text{-}C_3H_7OH + CH_3Cl$	3.78	−59.33	3.54	−59.09	2.85	−58.40	2.53	−58.08
av value and deviation[b]								−58.07 ± 0.11
1. $CHCl_2OH + CH_4 \rightarrow CH_3OH + CH_2Cl_2$	13.67	−66.69	11.90	−64.92	13.05	−66.07	12.91	−65.93
2. $CHCl_2OH + C_2H_6 \rightarrow C_2H_5OH + CH_2Cl_2$	8.19	−66.90	6.92	−65.63	7.48	−66.19	7.18	−65.89
3. $CHCl_2OH + C_2H_6 \rightarrow CH_3OH + CH_3CHCl_2$	7.80	−66.73	5.95	−64.83	5.90	−64.83	4.43	−63.36
4. $CHCl_2OH + C_3H_8 \rightarrow C_2H_5OH + CH_3CHCl_2$	3.95	−66.14	2.70	−64.89	2.55	−64.74	1.48	−64.49
5. $CHCl_2OH + C_3H_8 \rightarrow n\text{-}C_3H_7OH + CH_2Cl_2$	8.24	−67.02	7.15	−65.93	7.57	−66.35	7.18	−65.96
av value and deviation[b]								−65.92 ± 0.03
1. $CCl_3OH + CH_4 \rightarrow CH_3OH + CHCl_3$	12.13	−66.52	10.01	−64.40	12.51	−66.90	11.58	−65.97
2. $CCl_3OH + C_2H_6 \rightarrow C_2H_5OH + CHCl_3$	6.66	−66.74	5.02	−65.10	6.94	−67.02	5.85	−65.93
3. $CCl_3OH + C_2H_6 \rightarrow CH_3OH + CH_3CCl_3$	6.16	−68.01	4.14	−65.99	4.26	−66.11	1.29	−63.14
4. $CCl_3OH + C_3H_8 \rightarrow C_2H_5OH + CH_3CCl_3$	2.30	−67.41	0.89	−66.00	0.90	−66.01	−1.66	−63.45
5. $CCl_3OH + C_3H_8 \rightarrow n\text{-}C_3H_7OH + CHCl_3$	6.71	−66.86	5.25	−65.40	7.03	−67.18	5.85	−66.00
av value and deviation[b]								−65.96 ± 0.03

[a] Reaction enthalpies include thermal correction and zero-point energy. Units in kcal/mol. [b] Average value the deviation are based on selected reactions (see text) at the CBSQ//B3** level.

TABLE 8: Reaction Enthalpies at 298 K and Calculated Enthalpies of Formation[a]

	B3LYP/6-31G(d,p)		B3LYP/6-311+G(3df,2p)		QCISD(T)/6-31G(d,p)		CBSQ//B3LYP/6-31G(d,p)	
reaction series	ΔH°_{rxn}	ΔH°_{f298}	ΔH°_{rxn}	ΔH°_{f298}	ΔH°_{rxn}	ΔH°_{f298}	ΔH°_{rxn}	ΔH°_{f298}
1. $CHCl_2OH + C_2H_6 \rightarrow CH_2ClOH + C_2H_5Cl$	−0.30	−64.36	−0.41	−64.25	0.39	−65.05	0.99	−65.66
2. $CHCl_2OH + CH_4 \rightarrow CH_2ClOH + CH_3Cl$	3.69	−63.46	3.71	−63.49	4.81	−64.58	5.99	−65.77
3. $CHCl_2OH + CH_3Cl \rightarrow CH_2ClOH + CH_2Cl_2$	4.46	−65.76	3.61	−64.91	4.72	−66.01	4.64	−65.94
4. $CHCl_2OH + CH_3OH \rightarrow 2CH_2ClOH$	−5.51	−62.54	−4.58	−63.47	−3.53	−64.53	−2.27	−65.79
av value and deviation[b]								−65.79 ± 0.12
1. $CCl_3OH + C_2H_6 \rightarrow CH_2ClOH + CH_3CHCl_2$	−6.31	−62.60	−6.28	−62.64	−4.51	−64.40	−3.86	−65.05
2. $CCl_3OH + CH_4 \rightarrow CH_2ClOH + CH_2Cl_2$	−0.45	−62.56	−0.34	−62.67	2.63	−65.64	4.61	−67.62
3. $CCl_3OH + CH_3Cl \rightarrow CH_2ClOH + CHCl_3$	2.93	−65.60	1.72	−64.38	4.18	−66.84	3.31	−65.98
4. $CCl_3OH + CH_3OH \rightarrow CH_2ClOH + CHCl_2OH$	−14.12	−61.75	−12.24	−63.63	−10.42	−65.45	−8.29	−67.57
av value and deviation[b]								−66.56 ± 1.26

[a] Reaction enthalpies include thermal correction and zero-point energy. Units in kcal/mol. [b] Average value the deviation are based on four isodesmic reactions at the CBSQ//B3** level.

−66.56 ± 1.26 kcal/mol, which is 0.60 kcal/mol higher than the average CBSQ values of selected in Table 7.

We select CBSQ//B3** values from these three reaction series 1, 2, and 5 in Table 7 for our recommended values. The enthalpy of the pure enantiomer of lowest energy for dichloromethanol is −65.92 ± 0.76 kcal/mol and is −65.96 ± 0.76 kcal/mol for trichloromethanol.

The error limits of ΔH°_{f298} of three chlorinated methanols and radicals (see below) are estimated by adding the errors inherent in the present computational approach and the maximum uncertainties in the heats of formation of standard species in the working reactions.

Chloromethoxy Radicals. Table 9 shows the ΔH°_{f298} values for chloromethoxy radicals. The enthalpies are based on the ΔH°_{f298} of the above three chloromethanols and six isodesmic reaction series. Reaction series 3−6 are isodesmic, while reactions 1 and 2 are not. The enthalpy values for the three chloromethoxy radicals show excellent consistency at the CBSQ//B3** level for isodesmic reactions, where the standard deviation is within 0.02 kcal/mol. The DFT and QCISD(T) calculations for isodesmic reactions show a deviation of ca. ±1 kcal/mol with the CBSQ values. The DFT and QCISD(T) calculations result in larger variations for **non**isodesmic reaction series 1 and 2. CBSQ//B3** calculation results for nonisodesmic reactions are in satisfactory agreement with the isodesmic reactions but consistently result in 0.5 kcal/mol higher values for the three chloromethoxy radicals.

The recommended ΔH°_{f298} for the three chloromethoxy radicals are an average of the four isodesmic reactions at the CBSQ//B3** level: −5.13 ± 2.18, −7.65 ± 2.25, and −9.05 ± 2.24 kcal/mol for $CH_2ClO^\bullet$, $CHCl_2O^\bullet$, and $CCl_3O^\bullet$ respectively.

Hydroxychloromethyl Radicals. Table 9 also lists ΔH°_{f298} data for the hydroxychloromethyl radicals; all reactions are isodesmic. The CBSQ values show remarkable agreement across the six reaction series with a standard deviation on the order of 0.03 kcal/mol. The DFT and QCISD(T) also show good agreement; but somewhat more deviation, ca. ±1 kcal/mol. The recommended ΔH°_{f298} for the two hydroxychloromethyl radicals are an average over the six isodesmic reactions at the CBSQ//B3** calculation level and include the statistical distribution of rotation conformers: −14.46 ± 1.75 and −22.54 ± 1.83 kcal/mol for $C^\bullet HClOH$ and $C^\bullet Cl_2OH$, respectively.

Chloromethyl Radical. The results from one additional reaction scheme (reaction series 7 in Table 9) relate to the enthalpy of formation on $CH_2Cl^\bullet$ radical, for which reported values show significant disagreement; ΔH°_{f298} ranges from 27.7 ± 2[34b] to 29.1 ± 1.0[34c] kcal/mol. This scheme is hydroxychloromethyl radicals reacting with methyl chloride to produce methyl chloride radical and the corresponding chloromethanols. The ΔH°_{f298} values of hydroxychloromethyl radicals calculated by this reaction set at the CBSQ//B3** level give excellent agreement (maximum deviation of 0.03 kcal/mol from recommended values) when the experimental value (−27.7 ± 2 kcal/

TABLE 9: Reaction Enthalpies at 298 K and Calculated Enthalpies of Formation[a]

reaction series	B3LYP/6-31G(d,p) ΔH°_{rxn}	B3LYP/6-31G(d,p) ΔH°_{f298}	B3LYP/6-311+G(3df,2p) ΔH°_{rxn}	B3LYP/6-311+G(3df,2p) ΔH°_{f298}	QCISD(T)/6-31G(d,p) ΔH°_{rxn}	QCISD(T)/6-31G(d,p) ΔH°_{f298}	CBSQ//B3LYP/6-31G(d,p) ΔH°_{rxn}	CBSQ//B3LYP/6-31G(d,p) ΔH°_{f298}
1. $CH_2ClO^\bullet + CH_4 \rightarrow CH_3^\bullet + CH_2ClOH$	7.16	−12.52	3.79	−9.15	3.20	−8.56	−0.70	−4.66
2. $CH_2ClO^\bullet + C_2H_6 \rightarrow C_2H_5^\bullet + CH_2ClOH$	2.40	−11.43	−0.91	−8.12	0.22	−9.25	−4.36	−4.67
3. $CH_2ClO^\bullet + CH_4 \rightarrow CH_3O^\bullet + + CH_3Cl$	−0.30	−5.59	0.40	−6.29	−1.36	−4.53	−0.75	−5.14
4. $CH_2ClO^\bullet + C_2H_6 \rightarrow C_2H_5O^\bullet + CH_3Cl$	−0.50	−5.35	−0.01	−5.84	−1.27	−4.58	−0.69	−5.16
5. $CH_2ClO^\bullet + CH_3OH \rightarrow CH_3O^\bullet + CH_2ClOH$	8.90	−6.51	8.69	−6.30	6.97	−6.97	7.51	−5.12
6. $CH_2ClO^\bullet + C_2H_5OH \rightarrow C_2H_5O^\bullet + CH_2ClOH$	3.23	−6.49	3.29	−6.55	1.50	−4.76	1.85	−5.11
average value and deviation[b]								−5.13 ± 0.02
1. $CHCl_2O^\bullet + CH_4 \rightarrow CH_3^\bullet + CHCl_2OH$	1.86	−15.03	−1.21	−11.96	−1.87	−11.30	−6.02	−7.15
2. $CHCl_2O^\bullet + C_2H_6 \rightarrow C_2H_5^\bullet + CHCl_2OH$	−2.90	−13.94	−5.90	−10.94	−4.85	−11.99	−9.68	−7.16
3. $CHCl_2O^\bullet + CH_4 \rightarrow CH_3O^\bullet + CH_2Cl_2$	−5.61	−8.09	−4.60	−9.10	−6.43	−7.27	−6.07	−7.63
4. $CHCl_2O^\bullet + C_2H_6 \rightarrow C_2H_5O^\bullet + CH_2Cl_2$	−5.80	−7.86	−5.01	−8.65	−6.34	−7.32	−6.02	−7.64
5. $CHCl_2O^\bullet + CH_3OH \rightarrow CH_3O^\bullet + CHCl_2OH$	8.06	−8.90	7.30	−8.14	6.62	−7.46	6.83	−7.67
6. $CHCl_2O^\bullet + C_2H_5OH \rightarrow C_2H_5O^\bullet + CHCl_2OH$	2.39	−8.88	1.91	−8.40	1.15	−7.64	1.17	−7.66
average value and deviation[b]								−7.65 ± 0.02
1. $CCl_3O^\bullet + CH_4 \rightarrow CH_3^\bullet + CCl_3OH$	3.50	−16.75	0.45	−13.70	−1.14	−12.11	−4.68	−8.57
2. $CCl_3O^\bullet + C_2H_6 \rightarrow C_2H_5^\bullet + CCl_3OH$	−1.26	−15.66	−4.25	−12.67	−4.12	−12.80	−8.34	−8.58
3. $CCl_3O^\bullet + CH_4 \rightarrow CH_3O^\bullet + CHCl_3$	−3.97	−9.81	−2.94	−10.84	−5.70	−8.08	−4.73	−9.05
4. $CCl_3O^\bullet + C_2H_6 \rightarrow C_2H_5O^\bullet + CHCl_3$	−4.16	−9.58	−3.35	−10.39	−5.61	−8.13	−4.67	−9.07
5. $CCl_3O^\bullet + CH_3OH \rightarrow CH_3O^\bullet + CCl_3OH$	8.17	−10.38	7.07	−9.28	6.81	−9.02	6.85	−9.06
6. $CCl_3O^\bullet + C_2H_5OH \rightarrow C_2H_5O^\bullet + CCl_3OH$	2.50	−10.36	1.67	−9.53	1.33	−9.19	1.18	−9.04
average value and deviation[b]								−9.05 ± 0.01
1. $C^\bullet HClOH + CH_4 \rightarrow CH_3^\bullet + CH_2ClOH$	11.37	−16.73	10.24	−15.60	9.39	−14.75	9.15	−14.51
2. $C^\bullet HClOH + C_2H_6 \rightarrow C_2H_5^\bullet + CH_2ClOH$	6.61	−15.64	5.54	−14.57	6.41	−15.44	5.49	−14.52
3. $C^\bullet HClOH + CH_4 \rightarrow C^\bullet H_2OH + CH_3Cl$	9.99	−15.67	8.87	−14.55	9.44	−15.12	8.84	−14.52
4. $C^\bullet HClOH + C_2H_6 \rightarrow CH_3C^\bullet HOH + CH_3Cl$	2.50	−15.20	1.86	−14.56	2.88	−15.58	1.80	−14.50
5. $C^\bullet HClOH + CH_3OH \rightarrow C^\bullet H_2OH + CH_2ClOH$	0.79	−14.75	0.58	−14.54	1.11	−15.07	0.58	−14.54
6. $C^\bullet HClOH + C_2H_5OH \rightarrow CH_3C^\bullet HOH + CH_2ClOH$	−1.23	−14.06	−1.45	−13.84	0.11	−15.40	−0.74	−14.55
7. $C^\bullet HClOH + CH_3Cl \rightarrow CH_2Cl^\bullet + CH_2ClOH$	5.33	−16.10	4.10	−14.87	4.33	−15.10	3.76	−14.53
average value and deviation[b]								−14.52 ± 0.02
1. $C^\bullet Cl_2OH + CH_4 \rightarrow CH_3^\bullet + CHCl_2OH$	10.57	−23.74	9.96	−23.13	8.55	−21.72	9.34	−22.51
2. $C^\bullet Cl_2OH + C_2H_6 \rightarrow C_2H_5^\bullet + CHCl_2OH$	5.81	−22.65	5.27	−22.11	5.56	−22.40	5.68	−22.52
3. $C^\bullet Cl_2OH + CH_4 \rightarrow C^\bullet H_2OH + CH_2Cl_2$	13.65	−22.56	12.21	−21.12	13.32	−22.23	13.67	−22.58
4. $C^\bullet Cl_2OH + C_2H_6 \rightarrow CH_3C^\bullet HOH + CH_2Cl_2$	6.17	−22.10	5.19	−21.12	6.75	−22.68	6.64	−22.57
5. $C^\bullet Cl_2OH + CH_3OH \rightarrow C^\bullet H_2OH + CHCl_2OH$	−0.01	−21.76	0.31	−22.08	0.27	−22.04	0.77	−22.54
6. $C^\bullet Cl_2OH + C_2H_5OH \rightarrow CH_3C^\bullet HOH + CHCl_2OH$	−2.03	−21.07	−1.72	−21.38	−0.73	−22.37	−0.54	−22.56
7. $C^\bullet Cl_2OH + CH_3Cl \rightarrow CH_2Cl^\bullet + CHCl_2OH$	4.53	−23.11	3.83	−22.41	3.49	−22.07	3.95	−22.53
average value and deviation[b]								−22.54 ± 0.03

[a] Reaction enthalpies include thermal correction and zero-point energy. Units in kcal/mol. [b] Average value calculated at the CBSQ//B3** level, and the deviation are between the selected isodesmic reactions (see text).

TABLE 10: Energy Difference of the Conformers at the Four Calculation Levels, Relative Fraction, and Overall ΔH°_{f298}

	ΔE of conformers (kcal/mol)						
	B3LYP/6-31G(d,p)	B3LYP/6-311+G(3df,2p)	QCISD(T)/6-31G(d,p)	CBSQ//B3LYP/6−31G(d,p)	ΔH°_{f298}[e] (kcal/mol)	relative fraction	final ΔH°_{f298} (kcal/mol)
$CHCl_2OH$ (1)[a]					−65.92	0.9862	
$CHCl_2OH$ (2)[b]	3.68	2.98	3.11	2.94	−63.02	0.0069	−65.88 ± 0.76
$C^\bullet HClOH$ (1)[c]					−14.52	0.9710	
$C^\bullet HClOH$ (1)[d]	3.25	2.37	2.65	2.08	−12.44	0.0290	−14.46 ± 1.75

[a] The H−H anti conformer in $CHCl_2OH$. [b] The H−Cl anti conformer in $CHCl_2OH$. [c] The H−Cl gauche conformer in $C^\bullet HClOH$. [d] The H−Cl anti conformer in $C^\bullet HClOH$. [e] Enthalpy of formation at 298 K calculated at the CBSQ//B3LYP/6-31G(d,p) level.

mol) for the $CH_2Cl^\bullet$ radical is used. The recommended ΔH°_{f298}'s for hydroxychloromethyl radicals does not include the values from this reaction due to the large error range. The agreement between values derived with $CH_2Cl^\bullet$ in working reactions and the other isodesmic reaction values for each of the radicals in this study gives support to this ΔH°_{f298} (−27.7 kcal/mol) value for $CH_2Cl^\bullet$.

Enthalpy of Rotational Conformer. There are three staggered conformers in $CHCl_2OH$; two of them are H−Cl anti and one is H−H anti. For $C^\bullet HClOH$, there are two staggered conformers: one H−H anti and one is H−Cl anti. Total electronic energies including ZPVE and thermal correction to 298 K of the $CHCl_2OH$, $C^\bullet HClOH$ conformers are estimated at all four calculation levels. Energy differences between the conformers at the above levels are listed in Table 10. ΔH°_{f298} of the rotational conformers are determined from values calculated at the CBSQ//B3** level using isodesmic reaction schemes. The statistical distribution and overall ΔH°_{f298} of $CHCl_2OH$ and $C^\bullet HClOH$ are also listed in Table 10. As noted in the discussion on rotational barriers, the energy difference between the conformers decreases for the higher level calculations. The energy difference at the CBSQ//B3** level is used to calculate the statistical distribution of rotational conformers.

Bond Energy. RO−H, R−OH, R−H, and R−Cl bond dissociation energies are presented in Table 11. They are estimated using the ΔH°_{f298} values of chloromethanols and the corresponding radicals from this work; plus reference radicals (ΔH°_{f298} are listed in Table 5). The RO−H bond energy for monochloromethanol increases ca. 0.7 kcal/mol relative to that of methanol, while the RO−H bond energy for di- and trichloromethanol are both similar at ca. 5−6 kcal/mol above that of methanol. The second chlorine increases the O−H bond

TABLE 11: Bond Energies at 298 K[a]

reaction series	bond energy (kcal/mol)
RO−H	
$CH_3OH \rightarrow CH_3O^\bullet + H^\bullet$	104.28
$CH_2ClOH \rightarrow CH_2ClO^\bullet + H^\bullet$	105.04
$CHCl_2OH \rightarrow CHCl_2O^\bullet + H^\bullet$	110.33
$CCl_3OH \rightarrow CCl_3O^\bullet + H^\bullet$	109.01
R−OH	
$CH_3OH \rightarrow CH_3^\bullet + OH^\bullet$	92.33
$CH_2ClOH \rightarrow CH_2Cl^\bullet + OH^\bullet$	95.20
$CHCl_2OH \rightarrow CHCl_2^\bullet + OH^\bullet$	98.81
$CCl_3OH \rightarrow CCl_3^\bullet + OH^\bullet$	94.39
R−H	
$CH_3OH \rightarrow C^\bullet H_2OH + H^\bullet$	96.21
$CH_2ClOH \rightarrow C^\bullet HClOH + H^\bullet$	95.71
$CHCl_2OH \rightarrow C^\bullet Cl_2OH + H^\bullet$	95.44
R−Cl	
$CH_2ClOH \rightarrow C^\bullet H_2OH + Cl^\bullet$	83.02
$CHCl_2OH \rightarrow C^\bullet HClOH + Cl^\bullet$	80.34
$CCl_3OH \rightarrow C^\bullet Cl_2OH + Cl^\bullet$	72.34

[a] Enthalpy of formation at 298 K for reference radicals are listed in Table 5.

energy by 5 kcal/mol, but the third chlorine has essentially no effect. The increase in O−H bond energies may result from interaction between the electronegative chlorine on the methyl and electropositive hydroxyl hydrogen, as well as the increased electronegativity of the Cl(s) on the methyl further attracting the hydrogen's electron through the hydroxyl hydrogen bonding. Several recent studies[44−46] suggest significant hydrogen bonding interactions occur between C−Cl···H bonds. The stable conformations of di- and trichloromethanol both have the hydroxyl hydrogen gauche to two Cl's, so they have similar O−H bond energies.

The R−OH bond energies increase from 92.3 in $CH_3{-}OH$ to 98.8 in $CHCl_2{-}OH$ and then decrease to 94.4 kcal/mol in $CCl_3{-}OH$. The C−Cl bond energies decrease from 83.0 to 80.3 to 72.3 kcal/mol with successive addition of chlorine.

The C−H bond energies (at 298 K) in methanol and chloromethanols are quite similar. They show a very slight decrease from 96.2 to 95.4 from CH_3OH through $CHCl_2OH$ with the increased chlorine substitution. In contrast, the C−H bond energies in CH_3Cl, CH_2Cl_2, and $CHCl_3$ show a more monotonic decrease at 99.4, 98.4, and 95.3 kcal/mol, respectively. The $H{-}CH_2OH$ bond is about 3 kcal/mol weaker than the $H{-}CH_2Cl$ bond; a comparison relative to $CH_3{-}H$ shows there is ca. 8.6 vs 5.4 kcal/mol stabilization in CH_2Cl and $C^\bullet H_2OH$ relative to CH_3.

Entropy (S°_{298}) and Heat Capacity ($C_p(T)$'s ($300 \leq T/\mathrm{K} \leq 1500$)). S°_{298} and $C_p(T)$ calculation results using B3LYP/6-31G(d,p) determined geometries and harmonic frequencies are summarized in Table 12. TVR represent the sum of contributions from translation, external rotation, and vibrations for S°_{298} and $C_p(T)$'s. The scaled vibrational frequencies and moments of inertia are given in Tables 13 and 14. In Table 13, we compare values with both the experimentally measured frequencies by Kunttu et al.[2] and Wallington et al.[5] and those computed by Tyndall et al.[3] at the RHF/6-31G(d,p) level and by Wang et

TABLE 12: Ideal Gas-Phase Thermodynamic Properties[a]

species and symmetry no.		ΔH°_{f298} [b]	S°_{298} [c]	$C_p(300)$ [c]	$C_p(400)$	$C_p(500)$	$C_p(600)$	$C_p(800)$	$C_p(1000)$	$C_p(1500)$
CH_2ClOH	TVR[d]		63.09	11.43	13.65	15.68	17.39	20.03	21.97	25.07
	I.R.[e]		2.53	1.75	2.03	2.16	2.19	2.08	1.91	1.56
(1)	total[f]	−58.07 ± 0.69	65.62	13.18	15.68	17.84	19.58	22.11	23.88	26.63
	Schneider et al.[g]	−58.8 ± 5								
	NIST[h]	−55.50	71.5	12.45		16.92		21.27	23.26	26.40
$CHCl_2OH$	TVR[d]		69.60	14.68	17.13	19.06	20.55	22.68	24.14	26.39
	I.R.[e]		1.24	2.23	3.08	3.49	3.48	2.96	2.41	1.65
(1)	total[f]	−65.88 ± 0.76	71.00	16.91	20.21	22.55	24.03	25.64	26.55	28.04
	Schneider et al.[g]	−66.3 ± 5								
	NIST[h]	−66.40	72.5	16.50		20.60		24.02	25.40	27.64
CCl_3OH	TVR[d]		73.59	18.93	21.35	22.99	24.14	25.60	26.51	27.82
	I.R.[e]		3.84	1.71	1.60	1.48	1.37	1.24	1.16	1.08
(1)	total[f]	−65.96 ± 0.76	79.61	20.64	22.95	24.47	25.51	26.84	27.67	28.90
(3)	total[f]	−65.96 ± 0.76	77.43	20.64	22.95	24.47	25.51	26.84	27.67	28.90
	Schneider et al.[g]	−70.0 ± 5								
	NIST[h]	−66.20	79.2	20.19		24.02		26.68	27.54	28.92
$CH_2ClO^\bullet$	total [f]	−5.13 ± 2.18	64.68	12.18	14.27	15.99	17.38	19.42	20.86	23.00
(1)	Schneider et al.[g]	−4.4 ± 5								
	NIST[h]	−2.4	64.4	11.76		15.69		19.21	20.71	22.98
$CHCl_2O^\bullet$	total[f]	−7.65 ± 2.25	72.17	15.58	17.71	19.27	20.40	21.93	22.90	24.23
(1)	Schneider et al.[g]	−6.6 ± 5								
	NIST[h]	−4.1	71.6	15.03		18.75		21.62	22.64	24.13
$CCl_3O^\bullet$	total[f]	−9.05 ± 2.24	79.03	19.80	21.65	22.80	23.56	24.44	24.90	25.40
(1)	Schneider et al.[g]	−10.4 ± 5								
	NIST [h]	−4.4	78.4	19.23		22.40		24.33	24.78	25.38
$C^\bullet HClOH$	TVR [d]		63.99	11.28	13.08	14.57	15.74	17.46	18.69	20.67
	I.R.[e]		1.47	2.60	3.32	3.46	3.26	2.61	2.11	1.49
(1)	total [f]	−14.46 ± 1.75	65.72	13.88	16.40	18.03	19.00	20.07	20.80	22.16
	NIST [h]	−16.60	65.4	13.07		16.83		19.83	20.93	22.57
$C^\bullet Cl_2OH$	TVR [d]		71.03	14.51	16.36	17.68	18.64	19.91	20.72	21.93
	I.R.[e]		3.61	2.15	1.88	1.65	1.49	1.29	1.19	1.08
(1)	total [f]	−22.54 ± 1.83	74.64	16.66	18.24	19.33	20.13	21.20	21.91	23.01
	NIST [h]	−22.70	73.7	16.68		19.57		21.49	22.10	23.20

[a] Thermodynamic properties are referred to a standard state of an ideal gas of at 1 atm. One torsional frequency is excluded in the calculations of entropies and heat capacities. Instead, a more exact contribution from hindered rotations about the C−O bond is included. [b] Units in kcal/mol. [c] Units in cal/(mol K). [d] The sum of contributions from translations, external rotations, and vibrations. [e] Contribution from internal rotation about the C−O bond. [f] Symmetry number is taken into account ($-R$ ln(symmetry number)). [g] Reference 4. [h] Reference 6c, NIST web site.

TABLE 13: Vibrational Frequencies (cm^{-1})

species	ν_1	ν_2	ν_3	ν_4	ν_5	ν_6	ν_7	ν_8	ν_9	ν_{10}	ν_{11}	ν_{12}	source
CH_2ClOH	342	452	632	950	1116	1180	1326	1384	1493	3018	3121	3730	this work[a]
	343	432	694	941	1075	1166	1325	1356	1469	2976	3097	3652	Wallington[b]
	372	469	669	959	1096	1114	1231	1323	1393	2913	2981	3591	experimental[c]
			697	960	1083	1176	1318	1374				3646	experimental[d]
$CHCl_2OH$	268	316	439	479	650	681	1135	1220	1256	1387	3132	3701	this work[a]
	276	316	438	458	673	748	1089	1222	1238	1359	3074	3620	Wallington[b]
						740	1105		1221	1388		3611	experimental[d]
CCl_3OH	222	240	324	335	393	415	514	720	738	1141	1298	3690	this work[a]
	231	247	333	344	392	417	522	778	786	1094	1266	3606	Wallington[b]
								784	784	1113	1311	3604	experimental[d]
$CH_2ClO^\bullet$	374	642	650	1028	1139	1239	1302	2880	2920				this work[a]
	382	687	696	1043	1050	1287	1339	2870	2932				Wang et al.[e]
$CHCl_2O^\bullet$	263	310	396	597	646	1033	1104	1119	2850				this work[a]
	280	315	428	668	770	1027	1168	1214	2962				Hou et al.[f]
$CCl_3O^\bullet$	194	223	313	354	356	453	541	727	1175				this work[a]
$C^\bullet HClOH$	364	457	661	822	1151	1258	1349	3136	3708				this work[a]
	360	437	701	827	1123	1217	1326	3050	3484				Wang et al.[e]
$C^\bullet Cl_2OH$	262	318	381	465	569	774	1193	1272	3706				this work[a]
	274	328	380	466	607	834	1176	1258	3663				Hou et al.[f]

[a] Frequencies are calculated at the B3LYP/6-31G(d,p) level of theory scaled by 0.9806. [b] Frequencies are calculated at the MP2/6-31G(d,p) level by Wallington et al. Scaled by 0.94. [c] Infrared frequencies observed by Kunttu et al. [d] Infrared frequencies observed by Wallington et al. [e] Frequencies are calculated at the UMP2(full)/6-31G(d) level by Wang et al. Scaled by 0.93. [f] Frequencies are calculated at the UMP2=FU/6-31G(d,p) level by Hou et al. Scaled by 0.95.

TABLE 14: Moments of Inertia[a]

species	I_a	I_b	I_c
CH_2ClOH	45.86215	330.96314	360.61622
$CHCl_2OH$	267.95397	570.46659	796.29309
CCl_3OH	752.35282	759.41437	1089.13758
$CH_2ClO^\bullet$	36.78321	323.23443	348.60294
$CHCl_2O^\bullet$	250.72784	571.62340	794.25535
$CCl_3O^\bullet$	717.61395	752.40835	1115.44988
$C^\bullet HClOH$	34.40767	313.37790	343.41185
$C^\bullet Cl_2OH$	242.97421	565.15953	796.85596

[a] Optimized at the B3LYP/6-31G(d,p) level of theory. Units in amu-Bohr^2.

al.[9a] at the UMP2(full)/6-31G(d) level. One torsional frequency in Table 13 is omitted in calculation of entropies S°_{298} and heat capacities $C_p(T)$. Instead, a more exact contribution from hindered rotations is calculated. I.R. represents the contribution from internal rotation about the C$-$O bond for S°_{298} and $C_p(T)$'s.

Standard entropies also include correction from rotational conformers. This correction is calculated by the following formula for 1 mol of mixture:[42]

$$\Delta S_{\text{mixing}} = -R\sum n_i \ln(n_i)$$

where n_i is the equilibrium mole fraction of the ith form. ΔS_{mixing} represents the entropy of mixing of rotational conformations or optical conformations.

Table 12 list comparisons with previous ab initio calculation data. The calculation results show agreement for the enthalpy data (except CCl_3OH) estimated by isodesmic reactions at the MP4/6-31G(d,p) level reported by Schneider et al.[4] The results also show agreement for the enthalpy, entropy, and heat capacities of chlorinated methanols (except ΔH°_{f298} of CH_2ClOH) with the data from the NIST web site.[6c] The ΔH°_{f298} values of CH_2ClOH are reported to be -55.49 kcal/mol on the web site of Carl Melius,[6b] we have checked the geometry of CH_2ClOH reported on the same web site and find that the Cl$-$C$-$O$-$H dihedral angle of CH_2ClOH is 180°, corresponding to the maximum in our intramolecular rotation potential energy curve (see Figure 4). This is probably the reason the enthalpy of CH_2ClOH by Melius et al. is 2.58 kcal/mol higher than that calculated in this work.

Group Value. Group additivity[42] is a straightforward and reasonably accurate calculation method to estimate thermodynamic properties of hydrocarbons and oxygenated hydrocarbons;[47] it is particularly useful for application to larger molecules and codes or databases for thermochemical properties and reaction mechanism generation. We develop a set of chloro$-$oxy$-$hydrocarbon groups derived from the thermodynamic property data of three chlorinated methanols in this work. Values are reported for the groups C/Cl/H_2/O, C/Cl_2/H/O, and C/Cl_3/O derived from CH_2ClOH, $CHCl_2OH$, and CCl_3OH, respectively.

As an example, group values for ΔH°_{f298} and C_p's of C/Cl/H_2/O are calculated on the basis of

$$(CH_2ClOH) = (C/Cl/H_2/O) + (O/C/H)$$

and S°_{298} of C/Cl/H_2/O is calculated on the basis of

$$(CH_2ClOH) = (C/Cl/H_2/O) + (O/C/H) - R\ln(\sigma)$$

where $R = 1.987$ cal/(mol K) and σ is symmetry number. The group values of C/Cl_2/H/O and C/Cl_3/O are estimated in the same manner. Symmetry ($\sigma = 3$) is used for CCl_3OH. The group values for ΔH°_{f298}, S°_{298}, and $C_p(T)$ of O/C/H are taken from the existing literature data,[47] which come from alcohols. The carbon$-$chlorine$-$oxygen group values are derived in this work and are listed in Table 15. The group values for heat of formation decrease with an increased number of chlorine atoms, but not linearly. The carbon$-$chlorine$-$oxygen group values for entropy and heat capacities below 1500 K increase with an increased number of chlorines, as expected for the increased mass and lower vibrational frequencies.

Hydrogen Bond Increment Group Value for Radicals. A method to estimate thermochemical properties for radicals from the corresponding properties of the parent with a H atom bonded to the radical site using a single group to modify the parent properties (hydrogen bond increment (HBI) group) has been reported by Lay et al.[29] HBI group values are derived for the chloro$-$oxy radicals in this study, using the thermodynamic property data of chloromethoxy and hydroxychloromethyl radicals and parent chloromethanols. Increment values are

TABLE 15: Group Values

group	ΔH°_{f298} [a]	S°_{298} [b]	$C_p(300)$ [b]	$C_p(400)$	$C_p(500)$	$C_p(600)$	$C_p(800)$	$C_p(1000)$	$C_p(1500)$
O/C/H [c]	−37.90	29.07	4.30	4.50	4.82	5.23	6.02	6.61	7.44
$C/Cl/H_2/O$	−20.17	36.55	8.88	11.18	13.02	14.35	16.09	17.27	19.19
$C/Cl_2/H/O$	−27.98	41.93	12.61	15.71	17.73	18.80	19.62	19.94	20.60
$C/Cl_3/O$	−28.06	50.54	16.34	18.45	19.65	20.28	20.82	21.06	21.46

[a] Units in kcal/mol. [b] Units in cal/(mol K). [c] Reference 47.

TABLE 16: Hydrogen Bond Increment (HBI) Group Values

species	bond energy [a]	ΔS°_{298} [b]	$\Delta C_p(300)$ [b]	$\Delta C_p(400)$	$\Delta C_p(500)$	$\Delta C_p(600)$	$\Delta C_p(800)$	$\Delta C_p(1000)$	$\Delta C_p(1500)$
$CH_3O^\bullet$	104.28	−4.18	−0.88	−0.83	−1.02	−1.28	−1.79	−2.26	−3.16
$CH_2ClO^\bullet$	105.04	−0.94	−1.00	−1.41	−1.85	−2.20	−2.69	−3.02	−3.63
$CHCl_2O^\bullet$	110.33	1.17	−1.33	−2.50	−3.28	−3.63	−3.71	−3.65	−3.81
$CCl_3O^\bullet$	109.01	−0.58	−0.84	−1.30	−1.67	−1.95	−2.40	−2.77	−3.50
$C^\bullet H_2OH$	96.21	−2.15	0.44	0.34	−0.10	−0.67	−1.77	−2.68	−4.10
$C^\bullet HClOH$	95.71	0.10	0.70	0.72	0.19	−0.58	−2.04	−3.08	−4.47
$C^\bullet Cl_2OH$	97.44	3.64	−0.25	−1.97	−3.22	−3.90	−4.44	−4.64	−5.03

[a] Units in kcal/mol. [b] Units in cal/(mol K). Electronic spin degeneracy is included.

derived from calculated properties of $CH_2ClO^\bullet$, $CHCl_2O^\bullet$, $CCl_3O^\bullet$, $C^\bullet HClOH$, and $C^\bullet Cl_2OH$ and the respective parent−stable chloromethanols. A hydrogen atom bond increment (HBI) group for ΔH°_{f298} reflects the enthalpy change due to loss of a H atom[29] from a stable parent molecule in the form of the R−H bond energy. As an example, the bond energy of H−CHClOH is based on the heat of reaction of the following homolytic reaction:

$$(CH_2ClOH) = (CH_2ClO^\bullet) + H \qquad \Delta H^\circ_{rxn,\ 298} = D(CH_2ClO{-}H)$$

The bond energy of H−CHClOH can be written as

$$D(CH_2ClO{-}H) = (CH_2ClO^\bullet) + 52.1 - (CH_2ClOH)$$

ΔS°_{298} and ΔC_p are determined more directly, as the differences in respective properties of the molecule versus the radical in such a way that the HBI values for S°_{298} and $C_p(T)$ are added to the parent values to form the radical.

$$\text{radical} = \text{parent values} + \text{corresponding HBI value}$$

Heat capacity is the most straightforward, as it is a simple difference in the corresponding $C_p(T)$ properties:

$$C_p(T_i)\ CH_2ClO^\bullet = C_p(T_i)\ (CH_2ClOH) + \text{HBI}\ C_p(T_i)\ (CH_2ClO^\bullet)$$

Here we determine HBI $C_p(T_i)$ $(CH_2ClO^\bullet)$ values from the properties of the radical and parent. We note that the $C_p(T)$ and the S°_{298} components include contributions from vibration frequencies, moments of inertia, internal rotor(s), determined for the two species (parent and radical) for each respective radical.

The effects for changes in symmetry between the radical and parent are not included in the HBI group but are included in evaluation of the entropy of each species separately. The number of optical isomers does not change for these chloromethanol species (see below).

The HBI group value of ΔS°_{298} for $CH_2ClO^\bullet$ can be written as

$$\begin{aligned}\text{HBI}\ S^\circ_{298}(CH_2ClO^\bullet) &= [S^\circ_{298}(CH_2ClO^\bullet) + R\ \ln\sigma_{CH_2ClO^\bullet}] \\ &\quad - [S^\circ_{298}(CH_2ClOH) + R\ \ln\sigma_{CH_2ClOH}]\end{aligned}$$

Here σ represents symmetry or degeneracy and it is applied to both the radical and the parent molecule. Degeneracy of the radical electronic state is included in HBI group. Gain or loss of an optical isomer also needs to be considered in the entropy.

In general, effects of symmetry, optical isomers, and electron degeneracy need to be accounted for in the parent and radical species. Electronic degeneracy (R ln(2)) for one unpaired electron is included in the radical group. Symmetry and optical isomer effects are added to the target molecule (radical) when it is constructed, they are not included in the group. One exception is in hydroperoxy groups, where one additional optical isomer is present. The contribution from this OI is removed in the peroxy radical group, to account for loss of this optical isomer.

The group increment values for $CHCl_2O^\bullet$, $CCl_3O^\bullet$, $C^\bullet HClOH$, and $C^\bullet Cl_2OH$ are estimated in the same manner as $CH_2ClO^\bullet$ above. The tetrahedral structures result in σ (symmetry) of the radical species being 1, where rapid inversion eliminates the need to include a second optical isomer in $C^\bullet HClOH$ radical. The hydrogen bond group increment values for the radicals derived from chloromethanols are listed in Table 16.

As noted above the $C^\bullet HClOH$ radical has a tetrahedral structure and, with three different ligands, it will have two optical isomers. The inversion frequency is, however, only 364 cm^{-1}, and therefore we estimate interconversion between these isomers will be rapid on a time scale of measurement of light rotation measurement. We assign only one optical isomer to this $C^\bullet HClOH$ radical.

At first evaluation it may seem that these HBI groups are unique, that is, only applicable to the chloromethanol parent they were derived from, or to larger species through an ether link. We have noted in previous publications[29] that the hydrogen bond increment values result from changes in only a few frequencies and involve similar changes in structure for longer chain hydrocarbons. They are, therefore, appropriate as estimates for primary (terminal) chloro−oxy hydrocarbons. This will be further demonstrated in our ongoing work for primary and secondary chloro−oxy radical groups. We do note that bond enthalpies for the primary and secondary chloro−oxy radical groups will have the most significant differences, due to stabilization effects of added methyl groups. The R−H bond energies usually decrease in a trend similar to those of hydrocarbons changing from methyl (CH_3−H), to primary (C_2H_5−H), to secondary (C_2C−H), to tertiary (C_3C−H): 104.7, 101.6, 98.5, 96.5 kcal/mol, respectively.

Summary

Thermodynamic properties of chlorinated methanols and related radicals are calculated using density functional and ab initio methods with several reaction schemes for cancellation of errors. Standard enthalpies of formation, ΔH°_{f298}, are calculated using isodesmic reaction schemes based on the B3LYP/6-31G(d,p), B3LYP/6-311+G(3df,2p), QCISD(T)/6-31G(d,p), and CBSQ//B3LYP/6-31G(d,p) levels and include the statistical distribution of rotational conformers. Entropies, S°_{298}, and heat capacities ($C_p(T)$'s ($300 \leq T/\text{K} \leq 1500$)) are determined with B3LYP/6-31G(d,p) optimized geometries and frequencies, hindered internal rotation contributions to entropy and heat capacity are calculated by intramolecular torsion potential curves, and the entropy correction for mixing of rotational conformers is included. Enthalpy, entropy, and $C_p(T)$ properties are determined for C/Cl/H_2/O, C/Cl_2/H/O, and C/Cl_3/O chloro−oxy groups for use in group additivity. The group increment values for $CH_2ClO^\bullet$, $CHCl_2O^\bullet$, $CCl_3O^\bullet$, $C^\bullet HClOH$, and $C^\bullet Cl_2$-OH are also determined.

Enthalpies determined by the DFT, QCISD(T), and CBSQ calculations over several different working reaction schemes show remarkable precision for chlorinated methanols and hydroxychloromethyl radicals. The DFT and QCIST(T) methods show consensus for enthalpy of chloromethoxy radicals only in isodesmic reactions.

Acknowledgment. Many helpful discussions with Dr. Chuing-Ju Chen are acknowledged and we thank Chad Sheng for use of his SMCPS (Statistical Mechanics for Heat Capacity and Entropy) code to calculate S°_{298} and $C_p(T)$ terms plus ZPVE and thermal energy from Gaussian data files. This research is supported by the USEPA Northeast Regional Research Center and the USEPA Airborne Organics Research Center.

Supporting Information Available: Tables of total energies, ZPVE, and thermal correction to 298 K, and calculated rotation barriers for each rotational conformer of the three chlorinated methanols and two hydroxychloromethyl radicals and the coefficients of the Fourier expansion components, a_i and b_i, in eq F1. This material is available free of charge via the Internet at http://pubs.acs.org.

References and Notes

(1) (a) Lancar, I.; Le Bras, G.; Poulet, G. *J. Chim. Phys.* **1993**, *90*, 1897. (b) Atkinson, R. *J. Chem. Ref. Data* **1989**, Monograph 1.

(2) Kunttu, H.; Dahlqvist, M.; Murto, J.; Räsänen, M. *J. Phys. Chem.* **1988**, *92*, 1495.

(3) Tyndall, G. S.; Wallington, T. J.; Hurley, M. D.; Schneider, W. F. *J. Phys. Chem.* **1993**, *97*, 1576.

(4) Schneider, W. F.; Nance, B. I.; Wallington, T. J. *J. Am. Chem. Soc.* **1995**, *117*, 478.

(5) Wallington, T. J.; Schneider, W. F.; Barnes, I.; Becker, K. H.; Sehested, J.; Nielsen, O. J. *Chem. Phys. Lett.* **2000**, *322*, 97.

(6) (a) Kee, R. J.; Rupley, F. M.; Miller, J. A.; Sandia Nat. Lab Technol. Rep. SAND-87−8215B 1990; The Chemkin Thermodynamic Database. (b) Carl Melius, Sandia National Laboratories, unpublished data, August 1997, http://z.ca.sandia.gov/∼melius/bac/bac082897.eng0. (c) NIST species data, NIST web site with indication "reference not available". http://www.cstl.nist.gov/div836/ckmech/SpeciesData.html.

(7) Wallington, T. J.; Kaiser, E. W. *J. Phys. Chem.* **1994**, *98*, 5679.

(8) Wallington, T. J.; Orlando, J. J.; Tyndall, G. S. *J. Phys. Chem.* **1995**, *99*, 9437.

(9) (a)Wang, B.; Hou, H.; Gu, Y. *J. Phys. Chem. A* **1999**, *103*, 2060. (b) Hou, H.; Wang, B.; Gu, Y. *J. Phys. Chem. A* **1999**, *103*, 8075.

(10) Frisch, M. J.; Trucks, G. W.; Schlegel, H. B.; Gill, P. M. W.; Johnson, B. G.; Robb, M. A.; Cheeseman, R. J.; Keith, T.; Petersson, G. A.; Montgomery, J. A.; Raghavachari, K.; Al-Laham, M. A.; Zakrzewski, V. G.; Ortiz, J. V.; Foresman, J. B.; Cioslowski, J.; Stefanov, B. B.; Nanayakkara, A.; Challacombe, M.; Peng, C. Y.; Ayala, P. Y.; Chen, W.; Wong, M. W.; Andres, J. L.; Replogle, E. S.; Gomperts, R.; Martin, R. L.; Fox, D. J.; Binkley, J. S.; Defrees, D. J.; Baker, J.; Stewart, J. P.; Head-Gordon, M.; Gonzalez, C.; and Pople, J. A. *Gaussian 94*; Gaussian, Inc.: Pittsburgh, 1995.

(11) Lee, C.; Yang, W.; Parr, R. G. *Phys. Rev.* **1988**, *B37*, 785.

(12) Becke, A. D. *J. Chem. Phys.* **1993**, *98*, 5648.

(13) Montgomery, J. A.; Ocherski, J. W.; Petersson, G. A., *J. Chem. Phys*. **1994**, *101*, 5900.

(14) Scott, A. P.; Radom, L. *J. Phys. Chem.* **1996**, *100*, 16502.

(15) Lay, T. H.; Krasnoperov, L. N.; Venanzi, C. A.; Bozzelli, J. W. *J. Phys. Chem.* **1996**, *100*, 8240.

(16) Yamada, T.; Bozzelli, J. W. *J. Phys. Chem. A* **1998**, *102*, 7286.

(17) Yamada, T.; Bozzelli, J. W.; Berry, R. J. *J. Phys. Chem. A* **1999**, *103*, 5602.

(18) Sun, H.; Chen, C.-J.; Bozzelli, J. W. *J. Phys. Chem. A* **2000**, *104*, 8270.

(19) (a) Bair, R. A.; Goddard, W. A., III. *J. Am. Chem. Soc.* **1982**, *104*, 2719. (b) Omoto, K.; Marusaki, K.; Hirao, H.; Imade, M.; Fujimoto, H. *J. Phys. Chem. A* **2000**, *104*, 6499.

(20) Stryer, L. *Biochemistry*, 4th ed.; W. H. Freeman and Company: New York, 1995.

(21) Pauling, L. *The Nature of the Chemical Bond*; Cornell University Press: USA, 1947.

(22) Pedley, J. B.; Naylor, R. D.; Kirby, S. P. *Thermochemical Data of Organic Compounds*, 2nd ed.; Chapman and Hall: London, New York, 1986.

(23) Cox, J. D.; Pilcher, G. *Thermochemistry of Organic & Organometallic Compounds*; Academic Press: London, New York, 1970.

(24) Chase, M. W., Jr. *NIST-JANAF Thermochemical Tables*, 4th ed.; *J. Phys. Chem. Ref. Data* **1998**, Monograph 9.

(25) Frenkel. M.; Kabo. G. J.; Marsh K. N. *Thermodynamics of Organic Compounds in the gas state*; Thermodynamic Research Center, Texas A&M university: College Station, TX, 1994.

(26) Stull, D. R.; Westrum, E. F.; Sinke, G. C. *The Chemical Thermodynamic of Organic Compounds*; Robert E. Kireger Publishing Co.: Malabar, FL, 1987.

(27) Stull, D. R.; Prophet, H. *JANAF Thermochemical Tables*, 2nd ed.; U.S. Government Printing Office: Washington, DC, 1970.

(28) Marshall, P. *J. Phys. Chem. A* **1999**, *103*, 4560.

(29) Lay, T. H.; Bozzelli, J. W.; Dean, A. M.; Ritter, E. R. *J. Phys. Chem.* **1995**, *99*, 14514.

(30) Tsang, W., Martinho Simoes, J. A., Greenberg, A., Liebman, J. F., Eds. *Heats of Formation of Organic Free Radicals by Kinetic Methods in Energetics of Organic Free Radicals*; Blackie Academic and Professional: London, 1996.

(31) Berkowitz, J.; Ellison, G. B.; Gutman, D. *J. Phys. Chem.* **1994**, *98*, 2744

(32) Johnson, Russell D., III; Hudgens, J. W. *J. Phys. Chem.* **1996**, *100*, 19874.

(33) Mayer, P. M.; Glukhovtsev, M. N.; Gauld, J. W.; Radom, L. *J. Am. Chem. Soc.* **1997**, *119*, 12889.

(34) (a) Ruscic, B.; Berkowitz, J. *J. Phys. Chem.* **1993**, *97*, 11451. (b) Holmes, J. L.; Lossing, F. P. *J. Am. Chem. Soc.* **1988**, *110*, 7343. (c) Tschuikow-Roux. E.; Chen, Y. *J. Am. Chem. Soc.* **1989**, *111*, 9030. (c) Tschuikow-Roux, E.; Paddison, S. *Int. J. Chem. Kinet.* **1987**, *19*, 15.

(35) Dóbé, S.; Bérces, T.; Turányi, T., Márta, F.; Grussdorf, J.; Temps, F., Wagner, H. Gg. *J. Phys. Chem.* **1996**, *100*, 19864.

(36) Alfassi, Z. B.; Golden, D. M. *J. Phys. Chem.* **1972**, *76*, 3314.

(37) (a) Holmes, J. L.; Lossing, F. P.; Mayer, P. M. *J. Am. Chem. Soc.* **1991**, *113*, 9723.

(38) (a) Dyke J. M., Groves, A. P.; Lee, E. P. F.; Niavaran, M. H. Z. *J. Phys. Chem. A* **1997**, *101*, 373. (b) Block, D. A.; Armstrong, D. A.; Rauk, A. *J. Phys. Chem. A* **1999**, *103*, 3562.

(39) Ervin, K. M.; Gronert, S.; Barlow, S. E.; Gilles, M. K.; Harrison, A. G.; Bierbaum, V. M.; DePuy, C. H.; Lineberger, W. C.; Ellison, G. B. *J. Am. Chem. Soc.* **1990**, *112*, 5750.

(40) Curtiss, L. A.; Lucas, D. J. Pople, J. A. *J. Chem. Phys.* **1995**, *102*, 3292.

(41) Yamada, T.; Bozzelli, J. W.; Lay, T. H. *J. Phys. Chem. A* **1999**, *102*, 7646.

(42) Benson. S. W. *Thermochemical Kinetics*, 2nd ed.; Wiley-Interscience: New York, 1976.

(43) Jungkamp, Tim P. W.; Seinfeld, J. H. *Chem. Phys. Lett.* **1996**, *257*, 15.

(44) Aakeröy, C. B.; Evans, T. A.; Seddon, K., R.; Pálinkó, I. *New. J. Chem.* **1999**, (002), 145.

(45) Yoshida, H.; Harada, T.; Murase, T.; Ohno, K.; Matsuura, H. *J. Phys. Chem. A* **1997**, *101*, 1731.

(46) Tsuzuki, S.; Uchimaru, T.; Tanabe, K.; Hirano, T. *J. Phys. Chem.* **1993**, *97*, 1346.

(47) Cohen, N. *J. Phys. Chem. Ref. Data* **1996**, *25*, 1411.